https://doi.org/10.1016/j.tre.2021.102421

A NEW DAY-TO-DAY DYNAMIC NETWORK VULNERABILITY ANALYSIS APPROACH WITH WEIBIT-BASED ROUTE ADJUSTMENT PROCESS

Xiangdong Xu [a,b], Kai Qu [b], Anthony Chen [c*], Chao Yang [a,b]

[a] *Key Laboratory of Road and Traffic Engineering of the Ministry of Education, Tongji University, Shanghai, China*

[b] *Urban Mobility Institute, Tongji University, Shanghai, China*

[c] *Department of Civil and Environmental Engineering, The Hong Kong Polytechnic University, Kowloon, Hong Kong, China*

*Corresponding Author: Anthony Chen

E-mail: anthony.chen@polyu.edu.hk

ABSTRACT

The disruption of critical components in a transportation network can bring about severe network performance degradation and requires a relatively long period to recover, which would lead to commuters' day-to-day route choice adjustment. Under disruptions, there would be greater travel time variability (objective uncertainty) and travelers' perception error uncertainty (subjective uncertainty) in the transportation network. However, no vulnerability analysis method in the literature can consider the day-to-day network performance fluctuation under uncertainties. In this paper, we develop a new day-to-day dynamic network vulnerability analysis approach that allows the consideration of day-to-day network performance fluctuation based on a new day-to-day dynamic model considering both objective travel time uncertainty and subjective perception error uncertainty. Compared to most existing day-to-day models that either adopt User Equilibrium (UE) or Logit-based route choice criterion, the new day-to-day model has two advantages: (1) the Weibit model is used to capture travelers' subjective perception error uncertainty, which does not have the perfect information assumption in the UE model, or the identically distributed perception error assumption in the Logit model; and (2) the mean-excess travel time (METT) concept is used to capture the objective travel time uncertainty, which handles the inconsideration of travel time variability in most day-to-day models while remaining computational tractability. Based on the proposed day-to-day dynamic model, we develop a new component importance metric for network vulnerability analysis. This new metric characterizes the post-disruption day-dependent consequences to alleviate the limitation of only assessing the final static equilibrium consequence as in the existing studies of vulnerability analysis. Numerical examples are provided to demonstrate the features of the proposed day-to-day dynamic model and the new component importance metric, as well as their applicability in identifying the critical bridges in the Winnipeg network. The proposed approach provides a new

* Corresponding author. Email address: anthony.chen@polyu.edu.hk (A. Chen).

decision support tool for planners and managers in assessing the consequences of disruptions, identifying the critical components, and determining the recovery schedules after disruptions.

Keywords: Vulnerability; uncertainty; day-to-day dynamics; Weibit; mean-excess travel time

1 INTRODUCTION

1.1 Motivations and Observations

(1) Transportation Network Vulnerability Analysis

Transportation system is one of the important lifelines that are vital to people's health, safety, comfort, and economic activities. In light of the recent man-made and natural disasters frequently occurred in the world, disruptions to the transportation system can seriously damage the economic productivity of the society and cause inconvenience to peoples' daily life. These man-made and natural disasters have emphasized the multi-faceted importance and vulnerability of the transportation networks to the society, and the need for government agencies and communities to prepare strategies to identify and strengthen the weakness of transportation networks to withstand losses caused by these disruptive events.

Vulnerability analysis is a powerful tool in identifying the critical components in transportation networks. Among the abundant studies on transportation network vulnerability analysis, the two widely cited definitions of vulnerability come from Berdica (2002) and D'Este and Taylor (2003). Berdica (2002) defined vulnerability as the susceptibility of a system to threats and incidents that result in operational degradation, while D'Este and Taylor (2003) used the notion of accessibility to define that a network link is vulnerable if the loss of the link significantly diminishes the accessibility of the network. According to Taylor (2017), the main task of vulnerability analysis is to determine the network components (e.g., nodes and links), whose failures or degradations could significantly affect travelers' behaviors and network performance. Therefore, vulnerability analysis is also known as the identification of the weakest/critical/important/vulnerable components. This identification task has wide applications in both the pre-disaster planning and post-disaster management (e.g., targeted protection or retrofitting, strategic location of rapid response and repair stations, evacuation route planning, and evacuation network monitoring) to ensure that the critical components of the network are adequately monitored and protected.

Transportation network vulnerability analysis has received a great deal of attention in the past decade. Different perspectives, measures, and evaluation methods have been proposed to study the transportation network vulnerability (see, e.g., Chen *et al*., 2007a,b; Murray and Grubesic, 2007; Nagurney and Qiang, 2010; Luathep *et al*., 2011; Chen *et al*., 2012; Ho *et al*., 2013; El-

Rashidy and Grant-Muller, 2014; Gedik *et al*., 2014; Jenelius and Mattsson, 2015; Reggiani *et al*., 2015; Oliveira *et al*., 2016; Wang *et al*., 2016a; Bell *et al*., 2017; Calatayud *et al*., 2017; Bababeik *et al*. 2018; Haghighi *et al*., 2018; García-Palomares *et al*., 2018; Xu *et al*., 2018b; Gu *et al*., 2020). As reviewed by Mattsson and Jenelius (2015) and Xu *et al*. (2018b), most existing methods of transportation network vulnerability analysis are based on enumerating/generating/simulating disruption scenarios and then evaluating the network performance based on some performance measures (e.g., origin-destination (O-D) connectivity, total system cost, efficiency, and accessibility). The most widely used model in vulnerability analysis is the classical (static) user equilibrium (UE) traffic assignment model. To the best knowledge of the authors, *very few studies used within-day or day-to-day dynamic traffic assignment models in the network vulnerability analysis*. Jenelius (2007) and Cats and Jenelius (2014) considered the dynamics and information effects in the vulnerability analysis of road networks and transit networks, respectively. The "dynamics" considered in their studies belong to the within-day or short-term dynamics, which may be more applicable to the disruptions whose impact period and the subsequent recovery process are within a few hours. However, many disruptions in the transportation network are usually associated with severe infrastructure damages and a relatively long-term reconstruction process (from a few weeks to a few months). Such disruptions and reconstructions will cause the travelers' day-to-day route or mode choice adjustment afterwards. For example, on May 23, 2016, a truck accident damaged a four-lane segment in the Middle-Ring elevated expressway of Shanghai and also blocked its corresponding surface roads. The reconstruction lasted 14 days. This expressway segment accommodated daily traffic of more than 61,000 vehicles, whose route choices had to be adjusted after this truck accident (Tian and Chen, 2019). Empirical studies have also revealed that the traffic flow conditions of many elevated expressways and surface roads fluctuated dramatically during these 14 days and also afterwards (e.g., Li, 2018; Wang, 2019). *Hence, it is important and necessary to explicitly model the day-to-day route choice adjustment in the transportation network vulnerability analysis*.

Other than the characteristics of the considered disruption mentioned above, the widely-used static UE traffic assignment has the following drawbacks in the transportation network vulnerability analysis: (1) The existence or attainability of this theoretically ideal UE state has been questioned by many studies (e.g., Iida *et al*., 1992; Friesz *et al*., 1994). Instead, the network flows evolve from one realizable disequilibrium state to another; and (2) Managers may activate some recovery strategies far earlier than the long-term "final equilibrium" state after the disruption, which means that it is more meaningful to understand the evolution process rather than just the "final equilibrium" state. Ignoring the post-disaster network flow evolution process

may underestimate the negative consequences, and potentially lead to bias or cost-ineffectiveness in the recovery strategy decision-making as well as the inability of differentiating the impact of various recovery schedules.

(2) Day-to-Day Dynamic Traffic Assignment

As mentioned above, the disruption of a network component is likely to cause fluctuations of the transportation network states (including both supply and demand) and change commuters' route choice decisions from one day to another. To evaluate the system-wide performance after the disruption, an appropriate day-to-day dynamic traffic assignment model is needed to predict the network flow evolution.

Day-to-day dynamic traffic assignment models have been extensively studied in the literature. They can be classified into different categories according to different dimensions, such as discrete-time models versus continuous-time models, link-based models versus path-based models, and deterministic models versus stochastic models. For a more comprehensive review on day-to-day models, readers may refer to Cantarella and Watling (2016) and Zhou *et al*. (2017).

In this paper, we classify the current day-to-day models according to two dimensions: route choice criterion and uncertainty consideration (i.e., subjective and objective uncertainty). Herein the subjective uncertainty is referred to as the travelers' perception error due to their imperfect knowledge about the network states. The objective uncertainty is referred to as the travel time variability that widely exists in transportation systems. In reality, both subjective uncertainty and objective uncertainty affect the travelers' route choice decisions, especially after significant disruptions. Table 1 provides a selective summary of the existing models.

From Table 1, we can see that the existing studies mainly adopted either deterministic or Logit-based stochastic UE (SUE) route choice models. Also, most of them usually assumed that the link travel times on each day are deterministic without uncertainty. On the one hand, the unrealistic perfect information assumption of the deterministic UE model and the independently and identically distributed (IID) perception error assumption in the Logit-based SUE model, have been widely recognized and criticized by both researchers and practitioners. On the other hand, these models ignore the travel time variability that widely exists in daily travel. Many factors can contribute to the travel time variability, e.g., adverse weather, traffic incidents and accidents, work zone, special events, infrastructure disruption, etc. Empirical studies (e.g., Abdel-Aty *et al*., 1995) have revealed that travel time variability plays an important role in travelers' route choice decisions, and it is either the most or second most important factor for

most commuters. *Very few studies have considered both objective and subjective uncertainties simultaneously in the day-to-day dynamic models*.

Table 1 A selective summary of the existing day-to-day dynamic traffic assignment models

Literature	Route choice criterion	Objective or subjective uncertainty considered
Smith (1983, 1984); Friesz *et al.* (1994); Zhang *et al.* (2001); Yang and Zhang (2009); He *et al.* (2010); Han and Du (2012); Guo *et al.* (2013, 2015, 2016); Tan *et al.* (2015); Wang *et al.* (2015, 2016b); Xiao *et al.* (2016); Ye *et al.* (2018, 2021)	UE	None
Horowitz (1984); Cascetta (1989); Hazelton (2002); Hazelton and Watling (2004); Huang *et al.* (2008); Meneguzzer (2012); Bifulco *et al.* (2016); Lou *et al.* (2016); Rambha and Boyles (2016); Liu *et al.* (2017); Cheng *et al.* (2019); Xiao *et al.* (2019); Yu *et al.* (2020)	Logit-based SUE	Subjective uncertainty
Zhou *et al.* (2017)	Mixed UE and Logit-based SUE	Subjective uncertainty
Walting and Cantarella (2015); Cantarella and Watling (2016); Hazelton and Parry (2016)	Logit-based SUE	Subjective uncertainty and objective uncertainty (*)
This paper	Weibit-based SUE	Subjective uncertainty and capacity degradation (**)

Note:

*: belongs to stochastic day-to-day dynamic model; **: belongs to deterministic day-to-day dynamic model

Table 1 also shows that some limited studies indeed have developed stochastic day-to-day models to incorporate different sources of stochasticity, including the objective uncertainty such as demand or capacity uncertainty, and the subjective uncertainty such as random route choice behavior. Compared to deterministic models that assume the travelers' route choice mechanism per day is determined in advance, stochastic models consider uncertainty in travelers' route choice decisions and can provide the probability distribution of flow states (Watling and Cantarella, 2015; Cantarella and Watling, 2016; Hazelton and Parry 2016). Although stochastic models seem to be more general than deterministic models, the computational burden may hinder their applications in large-scale transportation networks. For example, Cantarella and Watling (2016) proposed a stochastic day-to-day model that considers Logit-based route choice and demand fluctuation, which was solved by Monte Carlo techniques due to the multinomial distribution of route flows. In addition, they still inherited the IID assumption of perception error due to the Logit-based route choice model. Note that the day-to-day dynamic network

vulnerability analysis addressed in this study needs to run a day-to-day dynamic model for each generated/enumerated disruption scenario.

Hence, to support the day-to-day dynamic network vulnerability analysis, it is necessary to develop a new day-to-day dynamic model that can reasonably capture the effects of both subjective perception error uncertainty and objective travel time uncertainty on the adjustment of travelers' route choice, while having computational tractability in large-scale networks.

1.2 Main Contributions of This Paper

Motivated by the above observations, this paper develops a new network vulnerability analysis method based on a day-to-day dynamic model under uncertainties. The proposed method includes the following two parts.

Part I- Modeling day-to-day dynamics under uncertainties: We explicitly model two types of uncertainties simultaneously in the day-to-day dynamic model: objective uncertainty due to travel time variability, and subjective uncertainty due to the travelers' imperfect knowledge about the network states. For the objective uncertainty, we use the mean-excess travel time (METT) concept (Chen and Zhou, 2010) as the travel cost to capture travelers' risk-averseness against travel time variability. For the subjective uncertainty, we provide a new exploration using an advanced discrete choice model (i.e., the Weibit model with the Weibull perception error distribution) to alleviate the drawbacks of the Logit model. With the Weibit model, we can capture the route-specific perception variance in the route adjustment process, rather than assuming a fixed and constant perception variance among different routes as in the Logit model. Then, the objective uncertainty and subjective uncertainty are integrated into the day-to-day modeling framework. Mathematical properties of the proposed model are also examined.

Part II- Day-to-day dynamic network vulnerability analysis: In evaluating the consequence of disruption scenarios, the existing (static) vulnerability analysis methods based on the static UE or Logit-SUE model only consider the consequence at the final equilibrium state, thus leading to the abovementioned drawbacks. To alleviate these drawbacks, we apply the proposed day-to-day dynamic model to develop a new metric of component importance for network-wide vulnerability analysis. Methodologically, the area circled by the network performance evolution curve derived by the proposed model and the pre-disruption normal network state is quantified. This new metric allows the consideration of both the performance dimension and time dimension, i.e., day-dependent consequence rather than the final equilibrium state. A case study in the realistic Winnipeg network is conducted to demonstrate the advantages of the proposed new

metric in identifying the critical bridges.

In summary, the **main contributions** of this paper are twofold: (1) the development of a day-to-day dynamic model considering both subjective perception error uncertainty (via the Weibit model) and objective travel time uncertainty (via the METT concept) to alleviate the drawbacks of the current day-to-day models that mostly adopt UE or Logit-based route choice criterion as well as ignore the travel time variability, and (2) the development of a component importance metric for day-to-day dynamic network-wide vulnerability analysis by characterizing the post-disruption day-dependent consequence to alleviate the limitations of only considering the final static equilibrium consequence as in the existing studies of vulnerability analysis.

The remainder of this paper is organized as follows. Section 2 presents the day-to-day dynamic model under uncertainties. Section 3 provides a new importance measure for network vulnerability analysis. Section 4 uses numerical examples to demonstrate the features of the proposed model and the new importance measure for network vulnerability analysis. Finally, conclusions and future research directions are summarized in Section 5. The notations and their explanations in this paper are summarized in Table D.1 in the Appendix D.

2 Modeling Day-To-Day Dynamics under both Subjective and Objective Uncertainties

In this section, we review two classical day-to-day dynamic traffic assignment models and then provide the proposed model under uncertainties.

2.1 Reviews of Two Classical Day-to-Day Dynamic Traffic Assignment Models

Consider a road network $G = [N, A]$, where N is the set of nodes, and A is the set of directed links. Let W denote the set of O-D pairs, and R^w is the set of routes between O-D pair w.

In this paper, the discrete day-to-day dynamic model is adopted, because it can better reflect the reality than the continuous-time day-to-day models (Watling and Hazelton, 2003). A generic discrete day-to-day route flow dynamic model can be expressed as follows:

$$\mathbf{f}^{(k+1)} = \left(1 - \alpha^{(k)}\right) \cdot \mathbf{f}^{(k)} + \alpha^{(k)} \cdot \mathbf{y}^{(k)}, \tag{1}$$

where $\mathbf{f}$ is the vector form of route flows, i.e., $\mathbf{f} = \{f_{w,r}, : r \in R^w, w \in W\}$, and $f_{w,r}$ is the traffic flow on route r that connects O-D pair w; $\mathbf{f}^{(k+1)}$ and $\mathbf{f}^{(k)}$ are the route flow patterns of day k+1 and day k; $\boldsymbol{y}^{(k)}$ is the target route flow pattern on day k+1 after travelers finish their travels

on day k; and $\alpha^{(k)}$ is the route flow adjustment ratio on day k.

On any day k, for any feasible route flow pattern, the travel demand conservation should be satisfied

$$\sum_{r \in R^w} f_{w,r}^{(k)} = q_w, \ \forall w \in W, \tag{2}$$

where q_w is the fixed travel demand of O-D pair w.

The path flow on day k should be non-negative, i.e.,

$$f_{w,r}^{(k)} \geq 0, \ \forall r \in R^w, w \in W, \tag{3}$$

Also, the flow on link a on any day k is the summation of all route flows that pass through the link on day k, i.e.,

$$v_a^{(k)} = \sum_{w \in W} \sum_{r \in R^w} f_{w,r}^{(k)} \rho_{ra}^w, \ \forall a \in A, \tag{4}$$

where $v_a^{(k)}$ is the flow of link a on day k; and ρ_{ra}^w is the link-route incidence indicator: $\rho_{ra}^w = 1$ if link a is on route r between O-D pair w, and $\rho_{ra}^w = 0$ otherwise.

Note that different day-to-day traffic assignment models differ in their choices of target flows and adjustment ratios. In the literature, there are two widely used principles to obtain the target route flow pattern: the UE principle and the Logit principle.

(1) UE principle

The UE principle was proposed by Wardrop (1952), which is perhaps the most widely used route choice model in urban and regional transportation planning practices. It assumes that all travelers are rational in terms of preferring the lower travel time routes, have perfect knowledge of network travel times, and are able to identify the minimum travel time route. The resulting flow pattern of UE is that only the minimum cost routes are used, while the routes even with travel cost slightly greater than the minimum cost are not used. Beckmann *et al*. (1956) developed an equivalent convex programming formulation for the UE problem with the congestion effect. In the day-to-day dynamic models, the UE condition can be expressed as

$$g_{w,r}^{(k)} \begin{cases} = u_w^{(k)}, & \text{if } f_{w,r}^{(k)} > 0 \\ \geq u_w^{(k)}, & \text{if } f_{w,r}^{(k)} = 0 \end{cases}, \quad \forall r \in K^w, \quad w \in W, \tag{5}$$

where $g_{w,r}^{(k)}$ is the cost of route r between O-D pair w on day k, and $u_w^{(k)}$ is the minimum travel cost of O-D pair w on day k. The above UE principle essentially implies the all-or-nothing (AON)

loading under the given route cost pattern on day *k*.

(2) Logit-based SUE principle

The stochastic user equilibrium (SUE) suggested by Daganzo and Sheffi (1977) incorporates a random perception error term in the route utility to capture travelers' imperfect knowledge of travel times, so that travelers do not always end up picking the minimum travel time route as in UE model. Different distribution assumptions on the random perception error term lead to different specialized probabilistic route choice models. In the literature, the Logit model (Dial, 1971) is perhaps the most widely used SUE model due to its closed-form route choice probability expression. Specifically, the Logit route choice probability expression is:

$$P_{w,r}^{(k)} = \frac{\exp\left(-\varphi g_{w,r}^{(k)}\right)}{\sum_{p \in R^w} \exp\left(-\varphi g_{w,p}^{(k)}\right)}, \quad \forall r \in R^w, \quad w \in W, \tag{6}$$

where $P_{w,r}^{(k)}$ is the probability of choosing route *r* connecting O-D pair *w* on day *k*, and φ is the dispersion parameter. This model has two known drawbacks: (1) its inability to account for overlapping (or correlation) among routes, and (2) its failure to account for perception variance with respect to trips of different lengths (Sheffi, 1985). These drawbacks are due to the underlying assumptions that the random error terms are independently and identically distributed (IID) Gumbel variates with the same and fixed perception variance.

2.2 The Proposed Day-to-Day Dynamic Traffic Assignment Model under Uncertainties

In this section, we first provide the methods to model the objective and subjective uncertainties. Then, we introduce the proposed day-to-day dynamic traffic assignment model in detail.

2.2.1 Modeling Objective and Subjective Uncertainties

To simplify the notations, below we ignore the day index *k*.

(1) Modeling Objective Travel Time Uncertainty

In this study, we use the classical BPR (Bureau of Public Roads) function as the link performance function:

$$T_a = t_a^0 \left[1 + \gamma \left(\frac{v_a}{C_a}\right)^b\right], \tag{7}$$

where T_a and C_a are the link travel time and capacity of link a; t_a^0 is the link free-flow travel time (FFTT); γ and b are BPR parameters, which are usually set as 0.15 and 4 respectively. Different sources can contribute to the uncertainty of link travel time, such as FFTT, link capacity, and link flow.

We adopt the METT concept to capture travelers' risk strategy for hedging against travel time variability. The METT concept (i.e., the unreliability consideration) can be justified by the empirical studies (FHWA, 2006; van Lint *et al*., 2008). They found that the consequences of the late trips located at the tail of heavily skewed distribution may be much more serious than those of modest delays, and have a significant impact on both travelers and freight shippers and carriers.

The METT at the confidence level of δ is defined as the conditional expectation of travel time T_a exceeding the corresponding travel time budget (TTB) $\xi_a(\delta)$ (Chen and Zhou, 2010; Xu *et al*., 2017)

$$\eta_a(\delta) = E[T_a | T_a \geq \xi_a(\delta)], \tag{8}$$

where T_a is the random travel time on link a, and $\xi_a(\delta)$ is the minimum threshold that satisfies the following δ-reliability requirement, i.e.,

$$\xi_a(\delta) = \min\{\xi | \, Pr(T_a \leq \delta) \geq \delta\} = E[T_a] + \epsilon_a(\delta), \ \forall a \in A, \tag{9}$$

where $\epsilon_a(\delta)$ is a buffer time added to the mean travel time $E[T_a]$ to ensure the travel time reliability requirement for on-time arrivals at the confidence level δ.

Due to the sub-additivity of link METT (Xu *et al*., 2017), route travel cost can be obtained by summing up the link METT of the links making up the route:

$$c_{w,r} = \sum_{a \in A} \eta_a(\delta) \rho_{ra}^w, \quad \forall r \in R^w, \ w \in W, \tag{10}$$

Remark 1. The link-based METT has the following desirable features in day-to-day vulnerability analysis. First, it has no specific assumptions on link travel time distributions, and hence any suitable link travel time distribution functions from empirical studies can be adopted. Second, the additive route cost structure allows the day-to-day model to be solved in a computationally tractable manner, which is quite beneficial to the day-to-day dynamic network vulnerability analysis that involves the evaluation of a large number of disruption scenarios.

In this study, we consider the link capacity degradation as the source of travel time uncertainty. Link capacity degradation widely exists in transportation networks, which can be caused by traffic accidents/incidents, adverse weather conditions, road pavement deteriorations, etc. The consideration of the link capacity degradation is due to the fact that the link capacities of almost all links are subject to degradation every day, even for the non-disrupted links. Following Lo and Tung (2003) and Lo *et al*. (2006), we assume that link capacity follows the uniform distribution with a lower bound of $\theta_a C_a$ and an upper bound of C_a. The formulas of mean and variance of link travel time under the uniformly distributed link capacity assumption are provided in the

Appendix A. For characterizing link travel time uncertainty, we adopt the Lognormal distribution, which has been recommended as one of the most well-fitted travel time distribution by empirical studies (e.g., Emam and Al-Deek, 2006; Kaparias *et al*., 2008; Rakha *et al*., 2010; Chen *et al*., 2014; Shen *et al*., 2020). With the lognormal distribution characterization of link travel time, following Xu *et al*. (2017), the METT can be analytically derived.

(2) Modeling Subjective Perception Error Uncertainty

For the subjective uncertainty, we adopt the Weibit model (i.e., with the Weibull perception error distribution) to capture the route-specific perception variance in the route adjustment process rather than assuming a fixed and constant perception variance among different routes as in the Logit model. The route choice probability expression of the Weibit model is:

$$P_{w,r} = \frac{(g_{w,r})^{-\beta^w}}{\sum_{p \in R^w} (g_{w,p})^{-\beta^w}}, \quad \forall r \in R^w, \quad w \in W, \tag{11}$$

where $P_{w,r}$ is the probability of choosing route r connecting O-D pair w; and β^w is the shape parameter of Weibull random error distribution of O-D pair w. The relationship between O-D demand and route flow is:

$$f_{w,r} = P_{w,r} \cdot q^w, \quad \forall r \in R^w, \quad w \in W, \tag{12}$$

Recall that in the Logit model, the trip variance is calculated by $(\sigma_{w,r})^2 = \pi^2/(6\varphi^2)$. Therefore, given a certain value of φ, the trip variances of different routes are the same in the Logit model. In contrast, due to without the identically distributed perception error assumption, the Weibit model can resolve the issue of homogeneous perception variance in the Logit model, because the variance of a route is a function of the route cost $g_{w,r}$ (Castillo *et al*., 2008), i.e.,

$$(\sigma_{w,r})^2 = \left[\frac{g_{w,r}}{\Gamma\left(1+\frac{1}{\beta^w}\right)}\right]^2 \left[\Gamma\left(1+\frac{2}{\beta^w}\right) - \Gamma^2\left(1+\frac{1}{\beta^w}\right)\right], \tag{13}$$

where $\Gamma(\cdot)$ is the gamma function, i.e., $\Gamma(x) = \int_0^{+\infty} t^{x-1} e^{-t}\, dt$. Eq. (13) shows that routes with different costs have different perception variances, despite the shape parameter β^w is an O-D specific parameter. This is more reasonable, because travelers on the longer routes have larger perception variances than those on the shorter routes in reality (Sheffi 1985). Some recent empirical studies have also verified the superiority of the Weibit model in travel choice problems over the Logit model with real data (Kurauchi and Ido, 2017; Li *et al*., 2020; Tinessa *et al*., 2020; Wen *et al*., 2021).

According to Kitthamkesorn and Chen (2013, 2014), in the Weibit-SUE model, the route travel cost is a function of multiplicative link travel costs, i.e.,

$$g_{w,r} = \prod_{a \in \Upsilon_r} \tau_a \quad \forall r \in R^w, w \in W \tag{14}$$

where τ_a is the link travel cost on link a, which could be a function of link travel time T_a (i.e., $\tau_a = F(T_a)$), and is usually specified as an exponential function of link travel time, e.g., $\tau_a = e^{0.075T_a}$; and Υ_r is the set of links on route r connecting O-D pair w. Then, the Weibit-based SUE problem can be formulated as the following optimization problem (Kitthamkesorn and Chen, 2013) in the route domain:

[Weibit-based SUE]

$$\min_{\mathbf{f}} Z(\mathbf{f}) = \sum_{a \in A} \int_0^{\sum_{w \in W} \sum_{r \in R^w} f_{w,r} \rho_{ra}^w} \ln \tau_a(w) dw + \sum_{w \in W} \frac{1}{\beta^w} \sum_{r \in R^w} f_{w,r} (\ln f_{w,r} - 1) \tag{15}$$

subject to Eqs. (2) and (3).

To integrate the objective uncertainty into the Weibit model (subjective uncertainty), we assume the link cost function τ_a to be the exponential function of link METT, i.e., $\tau_a = e^{0.075\eta_a(\delta)}$. The multiplicative route cost structure in Eq. (14) seems to be computationally expensive. However, we can perform a logarithmic transformation to calculate $\ln g_{w,r}$ as a simple summation of $\ln \tau_a$ (i.e., $\ln g_{w,r} = \sum_{a \in \Upsilon_r} \ln \tau_a$). Note that in the case where each route only consists of a single link (i.e., each link is a route), route cost equals link METT.

2.2.2 The Proposed Day-to-Day Dynamic Model

(1) Overall Structure

After introducing how to model objective and subjective uncertainties, now we present our day-to-day dynamic model. As mentioned in Section 2.1, the difference among different discrete day-to-day dynamic traffic assignment models lies in the determination of the target route flow pattern and the flow adjustment ratio. This section will present these two aspects in detail.

The overall framework of the proposed day-to-day dynamic model under uncertainties is shown in Fig. 1. Since the proposed model uses the Weibit model to model subjective uncertainty and METT to model objective uncertainty, the proposed model is referred to as the Weibit-METT model hereinafter. We assume that the day-to-day dynamic model will finally evolve into the equilibrium state. This assumption is reasonable because the travelers' route choice behavior will stabilize after some time period (Zhou *et al.*, 2017). This assumption has also been widely used in the literature.

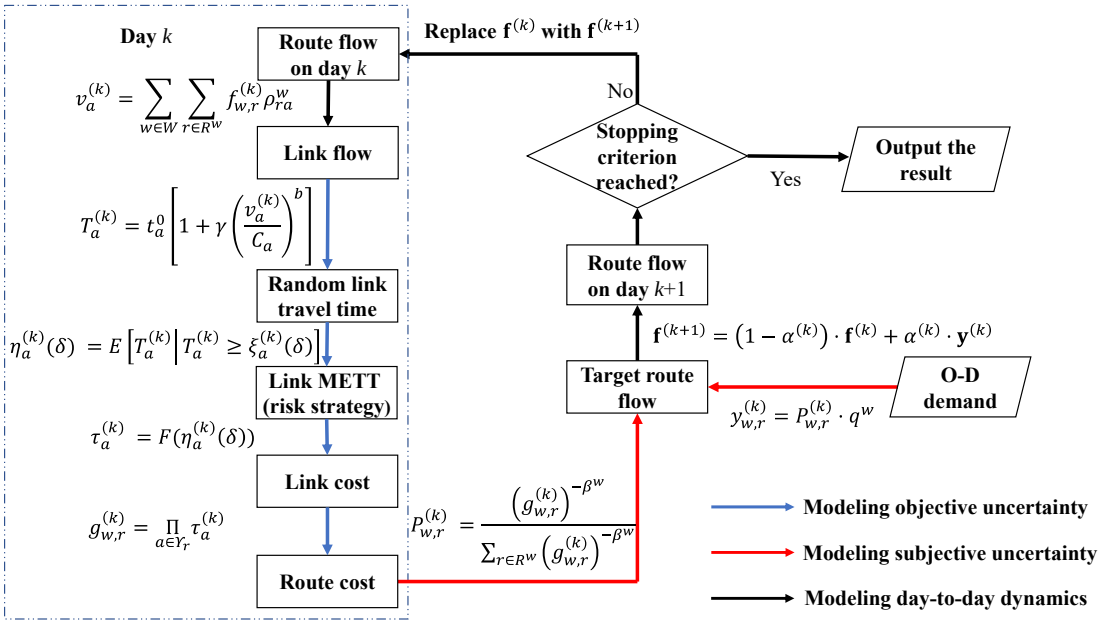

Fig. 1. The overall structure of the proposed day-to-day dynamic model under uncertainties

(2) Determination of the Target Flow Pattern

The motivation of travelers to adjust their route choice is due to their perception of an alternative route with less travel cost based on their latest travel experience. To capture the Weibit-based cost minimization behavior of travelers, we assume that the target flow is given by the following minimization problem named rational target flow assumption (RTFA).

[RTFA]:

$$\min_{\mathbf{f}\in\Omega}\sum_{w\in W}\sum_{r\in R^w}\ln g_{w,r}^{(k)}\cdot f_{w,r} + \sum_{w\in W}\frac{1}{\beta^w}\sum_{r\in R^w} f_{w,r}\cdot(\ln f_{w,r}-1) \tag{16}$$

where $\Omega = \{\mathbf{f}|\sum_{r\in R^w} f_{w,r} = q_w,\ f_{w,r}\geq 0,\ \forall r\in R^w,\ w\in W\}$.

Note that Zhou *et al.* (2017) proposed the RTFA based on the mixed UE and Logit-SUE model, which is different from Eq. (16). The RTFA in their study essentially implies the implementation of AON loading for travelers who follow the UE, and Logit loading for travelers who follow the Logit-based SUE on each day. In our study, Eq. (16) is the Weibit-based stochastic loading problem given the fixed route travel cost on day k, $\mathbf{g}^{(k)}$, which has a closed-form solution as shown in Eq. (17). The route cost herein reflects travel time variability via the METT.

$$y_{w,r}^{(k)} = q_w\frac{\left(g_{w,r}^{(k)}\right)^{-\beta^w}}{\sum_{r\in R^w}\left(g_{w,r}^{(k)}\right)^{-\beta^w}} \qquad \forall r\in R^w,\ w\in W \tag{17}$$

Therefore, the target route flow $\mathbf{y}^{(k)}$ reflects that travelers follow the Weibit-based route choice principle for their trips on the next day k+1. Travelers adjust their routes and choose the route with the minimum perceived cost. It is easy to see that the objective function of RTFA is strictly

convex, and the proposed day-to-day route flow dynamic model can produce a unique evolutionary trajectory. This means that the day-to-day evolution trajectory can be predicted in advance, which facilitates the day-to-day dynamic network vulnerability analysis in this paper.

Next, we discuss the relationship between the RTFA and the well-known rational behavior adjustment process (RBAP) proposed for the continuous day-to-day flow dynamic models (Zhang *et al*., 2001; Yang and Zhang, 2009; Zhou *et al*., 2017) in Proposition 1.

Proposition 1. If the current route flow pattern $\mathbf{f}^{(k)}$ is an optimal solution to [RTFA], then it is exactly the route flow pattern at the Weibit-SUE state. Otherwise, based on the current day's route travel costs, the total generalized travel time of the network will decrease on the next day $k+1$ if the route flows are adjusted according to Eq. (1), namely:

$$\tilde{\mathbf{g}}\left(\mathbf{f}^{(k)}\right)^{\mathrm{T}}\left(\mathbf{f}^{(k+1)}-\mathbf{f}^{(k)}\right)<0 \tag{18}$$

where $\tilde{\mathbf{g}}(\cdot)$ is the generalized cost operator. In the Weibit-SUE model of Eq. (15), the generalized cost is given by:

$$\widetilde{g_{w,r}}=\ln g_{w,r}+\frac{1}{\beta^{w}}\ln f_{w,r} \qquad \forall w\in W, r\in R^{w} \tag{19}$$

Proof. See Appendix B.

By comparing Eq. (18) to Zhang *et al*., (2009), one can find that Eq. (18) is a variation of the rational behavior adjustment process. The main difference lies in that here the Weibit-based generalized path cost operator is used (i.e., Eq. (19)) instead of the path cost operator. Therefore, we can infer that the proposed day-to-day dynamic model under the RTFA follows the rational behavior adjustment process. Note that the rational behavior adjustment process has been verified by Ye *et al*. (2018) with a virtual experiment.

(3) Determination of the Flow Adjustment Ratio

The establishment of the target flow determination strategy alone is not sufficient to ensure the convergence. Before presenting the flow adjustment ratio determination strategy, we present Proposition 2 as follows based on the property of RTFA.

Proposition 2. There exists $\overline{\alpha^{(k)}}\in(0,1]$ satisfying Eq. (20) and for any adjustment ratio $\alpha^{(k)}\in\left(0,\ \overline{\alpha^{(k)}}\right]$, $k=1,2,\ldots$, the proposed day-to-day dynamic model converges to the Weibit-SUE state.

$$\tilde{\mathbf{g}}\left((1-\alpha^{(k)})\mathbf{f}^{(k)}+\alpha^{(k)}\mathbf{y}^{(k)}\right)^{T}\left(\mathbf{y}^{(k)}-\mathbf{f}^{(k)}\right)\leq 0,\ \forall\alpha^{(k)}\in\left(0,\ \overline{\alpha^{(k)}}\right],\ k=1,2,\ldots \tag{20}$$

Proof. See Appendix C.

Proposition 2 indicates that, on each day k, after the target flow $\mathbf{y}^{(k)}$ is determined, if $\alpha^{(k)}$ takes a value satisfying Eq. (21), the proposed day-to-day dynamic model converges to the Weibit-SUE state.

$$\tilde{\mathbf{g}}\left((1-\alpha^{(k)})\mathbf{f}^{(k)}+\alpha^{(k)}\mathbf{y}^{(k)}\right)^{T}\left(\mathbf{y}^{(k)}-\mathbf{f}^{(k)}\right)\leq 0 \tag{21}$$

Based on this property, the flow adjustment determination strategy can be devised. For example, to find the set of $\alpha^{(k)}$ that satisfies Eq. (21) on each day, many line search methods can be used, such as the bisection method (Sheffi, 1985). For the details about calculating the flow adjustment ratio with the bisection method, please refer to Appendix C.

Remark 2. The strategy above is both behaviorally plausible and computationally tractable. First, the flow adjustment ratio $\alpha^{(k)}$ varies on a daily basis, unlike the typically used fixed constant (e.g., $\alpha^{(k)}=0.1$ for all days) which assumes that a predetermined and fixed proportion of travelers adjust their behaviors each day and hence lacks behavioral interpretation. Note that the flow adjustment ratio would vary day by day in the real world (Ye *et al*., 2018). To calibrate the day-dependent flow adjustment ratio in the real world, there are some previous studies that could be followed (e.g., Ye *et al*., 2018, Cheng *et al*., 2019). Second, similar to the Goldstein rule used in Zhou *et al*. (2017), the determination of flow adjustment ratio considers the recent network condition (including both flow and cost), and the feasible flow adjustment ratio on each day forms a continuous interval, rather than being a single or several discrete values. Therefore, it can provide reasonable behavioral justification. Besides, the calculation process associated with this strategy mainly involves calculating the generalized route cost in Eq. (19), which is much easier to perform than evaluating the objective function as in the Goldstein rule. Recall that the integral operation of METT makes the entire objective function quite complex.

In summary, the proposed discrete day-to-day dynamic model has the following important properties. First, the route flow evolution trajectory is unique. Second, the route flow pattern after convergence is equivalent to the Weibit-SUE state. Third, the determination strategies of target flow and flow adjustment ratio together guarantee that the adjustment process converges towards the Weibit-SUE state. For comparison purposes, a counterpart continuous day-to-day dynamic model is also established as shown in Appendix E, but we focus on the discrete day-to-day dynamic model in the following analysis.

3 DAY-TO-DAY DYNAMIC NETWORK VULNERABILITY ANALYSIS

As mentioned in Section 1, most existing studies of vulnerability analysis evaluate the consequence of a disruption scenario based on some performance measures at the final equilibrium state after the disruption. However, many disruptions (especially severe infrastructure damages) encountered in transportation systems have a long-term negative impact and also requires a long period to reconstruct and recover. Commuters' travel behavior would change after disruptions on a daily basis, and the network-wide performance may vary from one day to another. Ignoring the post-disaster network flow fluctuation may underestimate the negative consequences, and potentially lead to bias or cost-ineffectiveness in the recovery strategy decision-making as well as the inability of differentiating the impact of various recovery schedules.

Based on the day-to-day traffic assignment model proposed in Section 2, this section develops a new vulnerability evaluation metric by considering the day-to-day network performance fluctuation after the disruption of a network component.

Fig. 2 illustrates the proposed metric for network-wide vulnerability analysis. Consider that a disruption occurs at t_0, and the network performance degenerates to the lowest case and then recovers to an equilibrium state at t_1. The proposed metric is denoted by the area circled by the network performance evolution curve derived by the proposed day-to-day dynamic model and the curve of pre-disruption normal network state from t_0 (the occurrence time of the disruption) to t_1 (the recovered equilibrium state), as sketched in Fig. 2. We refer to the proposed metric as the dynamic network performance (DNP) measure. Mathematically, the general formula of DNP is

$$DNP = \int_{t_0}^{t_1} [NP(t_0) - NP(t)]\, dt \tag{22}$$

Eq. (22) is continuous with regard to t, and thus is applicable to the continuous day-to-day dynamic model in Appendix E. To fit in the proposed discrete day-to-day dynamic model, Eq. (22) can also be discretized as

$$DNP = \sum_{t=\{t_0+1, t_0+2, \ldots, t_1\}} \frac{|NP(t_0)-NP(t)|+|NP(t_0)-NP(t-1)|}{2} \tag{23}$$

In Eqs. (22) and (23), $NP(t_0)$ is the network performance on day t_0; $NP(t)$ is the network performance on day t, which is derived from the proposed day-to-day dynamic model. Traditionally, the metrics used in vulnerability analysis only focus on the network performance at the final equilibrium state, which is denoted by $NP(t_1)$ in Fig. 2. Note that the network performance evolution curve is similar to the resilience curve or triangle (Wan *et al.*, 2018; Zhou

et al., 2019) for characterizing the four dimensions of resilience, i.e., redundancy, robustness, rapidity, and resourcefulness. The main difference lies in that here the network performance at the new equilibrium state (i.e., $NP(t_1)$) is worse than the pre-disruption network performance (i.e., $NP(t_0)$) because no external interventions, such as the repairing procedure, are considered; while in the resilience curve, $NP(t_1)$ can be higher, lower or close to $NP(t_0)$ depending on the recovery schedule in question. In this study, we use DNP to identify the critical components of a network because it can consider the post-disaster network flow and performance fluctuation. The proposed method is not only limited to the case in which the equilibrium can be reached, but also is applicable to the case in which the equilibrium cannot be reached at the end of the investigated time horizon t_1. That is, to calculate the DNP metric within the specified time period (e.g., t_0 to t_1) resulting from different disruption scenarios, and then rank the disruption scenarios according to the metric.

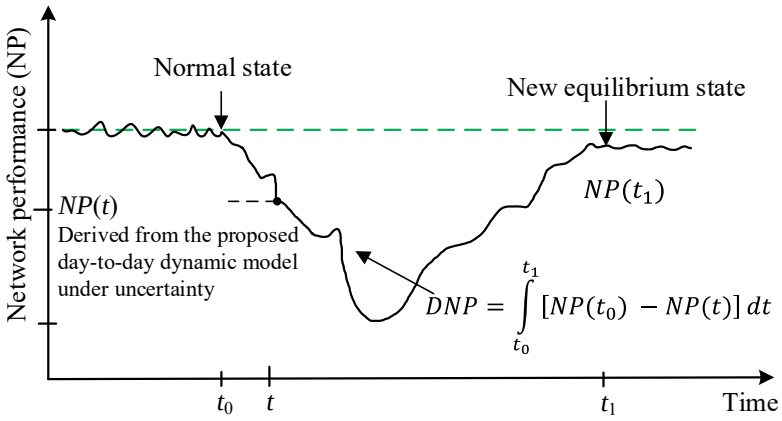

Fig. 2. Illustration of the proposed DNP metric for network-wide vulnerability analysis

In the literature, the total travel time (TTT), the sum of the product of link flow and link travel time of all links in the network (i.e., $TTT = \sum_{a \in A} v_a T_a$), has been one of the most widely used measures for assessing transportation network performance and design (Yang and Bell, 1998; Xu *et al.*, 2014; Yang *et al.*, 2017; Wang *et al.*, 2018). It has also been used as a typical performance measure in transportation vulnerability analysis (Taylor, 2017). In this study, considering the travel time variability, we use the expected value of TTT (ETTT) as the network performance measure. Note that ETTT has also been adopted as the network performance measure in network design problems under uncertainties (Chen and Yang, 2004). Since the traffic flow is deterministic in this paper, ETTT essentially equals the total expected travel time (TETT), namely the sum of the product of link flow and mean link travel time of all links in the network, i.e.,

$$ETTT = E(TTT)$$

$$= E\left(\sum_{a\in A} v_a T_a\right)$$

$$= \sum_{a\in A} v_a E(T_a) \ = TETT \tag{24}$$

Following the uniform link capacity distribution mentioned earlier, the mean link travel time $E(T_a)$ in Eq. (24) is calculated by Eq. (A.1) in this study.

4 NUMERICAL EXAMPLES

In this section, we use two networks to demonstrate the features of the proposed day-to-day dynamic model and the new metric for network vulnerability analysis. Specifically, network 1 (two-route network) is used to illustrate the advantages of the proposed day-to-day dynamic model. Network 2 (Winnipeg network) is used to demonstrate the property of the proposed metric for network vulnerability analysis.

4.1 Two-Route Networks

The two-route networks, shown in Fig. 3, are adopted to illustrate the property of the proposed day-to-day dynamic model from two aspects: the evolution process and the equilibrium state. Both networks consist of one O-D pair connected by two independent links/routes. The O-D demand of both networks is set to be 100, and the capacity of both links is 100. The free flow travel times of the two routes are 10 and 5 for the short network, and 125 and 120 for the long network. The parameters γ and b of the BPR function in Eq. (7) are set to be 0.15 and 4, respectively. The link capacity of both links is assumed to follow a uniform distribution with $\theta_a C_a$ as the lower bound and C_a as the upper bound.

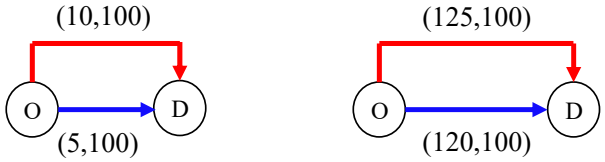

(Free flow travel time, capacity)

(a) Short network (b) Long network

Fig. 3 Two-route networks

The proposed Weibit-METT day-to-day dynamic model is compared with the other five day-to-day traffic assignment models to show its advantages. The other five day-to-day models are UE, Logit, Weibit, UE-METT, and Logit-METT/Logit-scaling(Logits)-METT models. For simplicity, we refer to UE, Logit, and Weibit models as BPR models, and UE-METT, Logit-METT, and Weibit-METT models as METT models hereinafter. Recall that since each link is a route in the two-route networks, route cost equals link METT in the METT models.

For a fair comparison, the coefficient of variation (CoV) of Logit-based models (including Logit and Logits-METT) and Weibit-based (including Weibit and Weibit-METT) models are all set to be 0.3. Under this value of CoV, the dispersion parameter φ of Logit-based models is 0.85503 and 0.03563 in the short and long networks, respectively; and Weibit models use β^w =3.7 in both networks. Besides, we adopt the same determination strategies of target flow (namely RTFA) and flow adjustment ratio for all the day-to-day models to guarantee a fair comparison. As for the initial flow pattern, we assume the O-D demand is equally assigned to the two paths.

4.1.1 Comparison among Weibit-METT, UE, and Logit Models

Recall that the majority of the existing day-to-day dynamic model uses either UE or Logit route choice principle. This example uses the short network shown in Fig. 3(a) to demonstrate the differences between the proposed Weibit-METT day-to-day dynamic model and the UE and Logit models. For the Weibit-METT model, we set θ_a= 0.6 and δ = 0.8.

The evolution curves of route flow and route cost are shown in Fig. 4 and Fig. 5, respectively. The results at the equilibrium state are presented in Table 2. We can easily verify the satisfaction of the corresponding equilibrium conditions. From Fig. 4 and Fig. 5, the three models converge within 10 days, due to the simple structure of the network. However, the flow evolution curves differ from each other. From Fig. 4, all travelers switch to route 2 on day 2 in the UE day-to-day model. Relative to that of the UE day-to-day model, the flow evolution curve of the Logit day-to-day model is closer to the proposed model due to their similar considerations of subjective uncertainty.

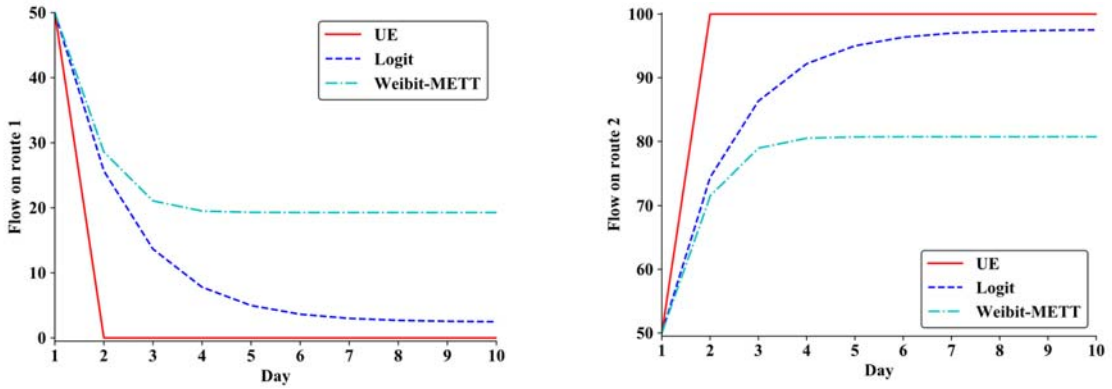

(a) Flow on route 1 (b) Flow on route 2

Fig. 4. The evolution process of route flow

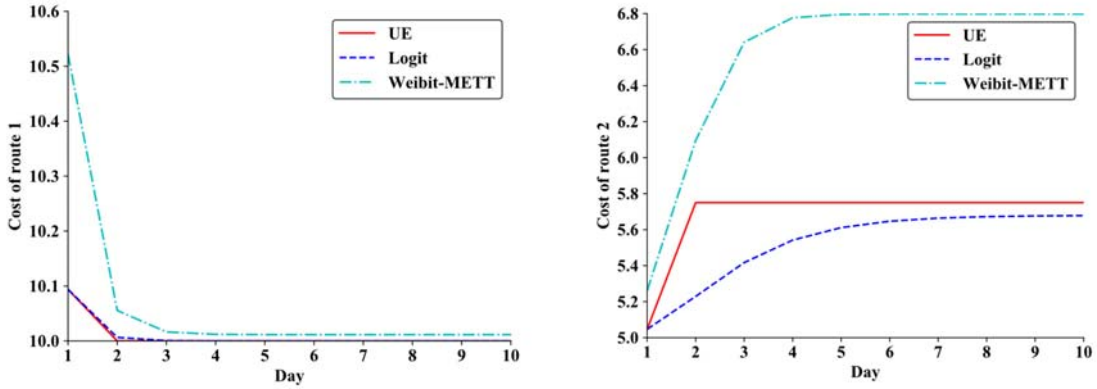

a) Cost of route 1 (b) Cost of route 2

Fig. 5. The evolution process of route cost

Table 2. Results of three models at the equilibrium state

Item	Model		
	UE	Logit	Weibit-METT
Flow on route 1	0	2.43	19.27
Flow on route 2	100	97.57	80.73
Cost of route 1	10	10 (12.21)	10.01 (3.10)
Cost of route 2	5.75	5.68 (12.21)	6.80 (3.10)

Note: The numbers in the parenthesis are the generalized route costs.

The difference in the flow assignment results among the three models can be explained by Fig. 6 and Fig. 7. The UE model considers neither subjective nor objective uncertainty, so it assigns all the demand on the shortest route (i.e., route 2). As for the Logit model, although it considers subjective uncertainty and hence allocates some flows on route 1, it assumes that the two routes have an identically distributed perception error with the same variance of 2.25 as shown in Fig. 6. Also, the Logit model ignores the objective uncertainty. By contrast, the Weibit-METT model considers both objective uncertainty and subjective uncertainty. First, as shown in Fig. 7 (a), due to the capacity degradation assumption, the actual travel time is randomly distributed rather than a fixed value as in the other two BPR models (i.e., UE and Logit). The variability in the actual travel time lies in that, while the actual travel time of route 1 has a larger mean than that of route 2 (10.01 versus 5.96), its variance is much smaller (1.39×10^{-5} versus 0.33). This is because the travel time variance is largely dependent on the flow (see Eq. (A.2) in the Appendix A). Second, as shown in Fig. 7 (b), unlike in the Logit model where the two routes have identical perception variance, the perception variance of route 1 is more than twice that of route 2 in the Weibit-METT model. Due to the above two factors, the flow gap between the two routes at the

equilibrium state is much smaller in the Weibit-METT model than in the other two models.

To sum up, under the same determination strategies of target flow and flow adjustment ratio, the above three models can converge to their respective equilibrium state within a short period. However, the results at the equilibrium state are quite different. This indicates that the improper consideration or ignorance of subjective uncertainty and/or objective uncertainty in the commonly used UE and Logit models may lead to biased results of flow assignment. Intuitively, the flow assignment bias would further influence the vulnerability analysis result.

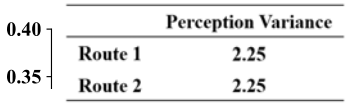

Fig. 6. Perceived travel cost distribution in the Logit model (subjective uncertainty)

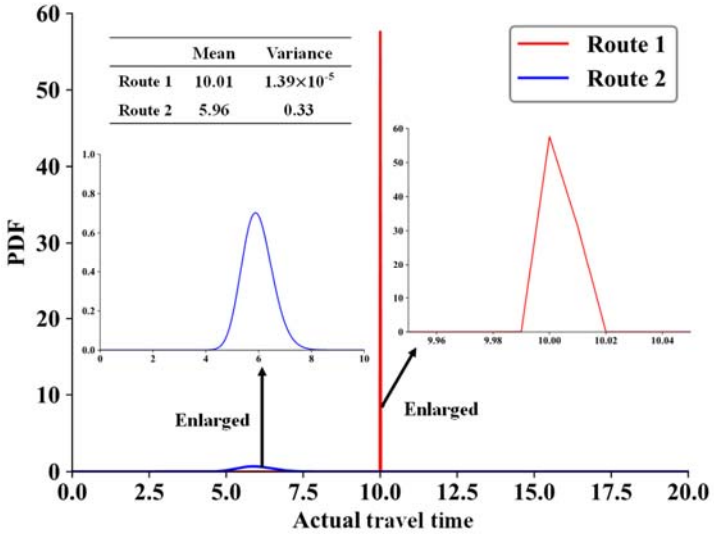

(a) Actual travel time distribution (objective uncertainty)

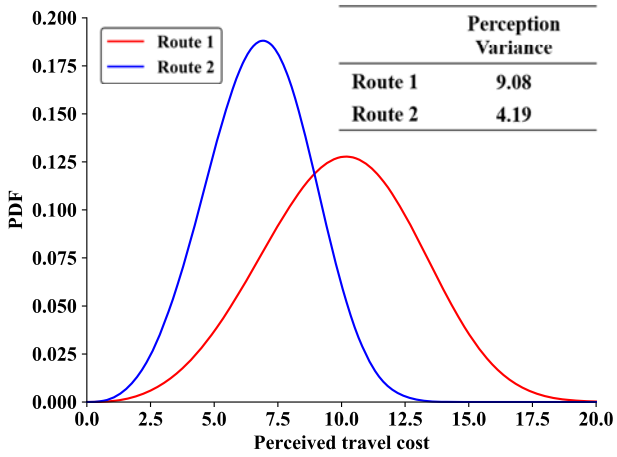

(b) Perceived travel cost distribution (subjective uncertainty)

Fig. 7. Distributions of actual travel time and perceived travel cost in the Weibit-METT model

4.1.2 Investigating the Effects of Objective Uncertainty and Subjective Uncertainty

In this section, we investigate the effects of objective uncertainty and subjective uncertainty on the flow pattern at the equilibrium state. First, we illustrate the effect of objective uncertainty by comparing the results produced by three METT models (i.e., UE-METT, Logit-METT, and Weibit-METT) with their corresponding BPR models (i.e., UE, Logit, and Weibit). Then, we show the advantage of Weibit model in characterizing subjective uncertainty by comparing the results of Weibit-METT model with those of UE-METT and Logit-METT models.

4.1.2.1 Comparison between METT models and BPR counterparts

The main difference between the two categories of models is that the METT models take into consideration the objective uncertainty (via link capacity lower bound θ_a) as well as travelers' attitudes towards risks (via confidence level δ).

The following two experiments are conducted to show the impacts of θ_a and δ, respectively. We still consider the short network shown in Fig. 3(a). First, we fix θ_a at 0.5, and vary δ from 0.5 to 0.9 with an interval of 0.1. Then, we fix δ at 0.8 and vary θ_a from 0.1 to 0.9 with an interval of 0.2. The flow assignment results of route 2 from the two experiments are shown in Fig. 8 and Fig. 9, respectively.

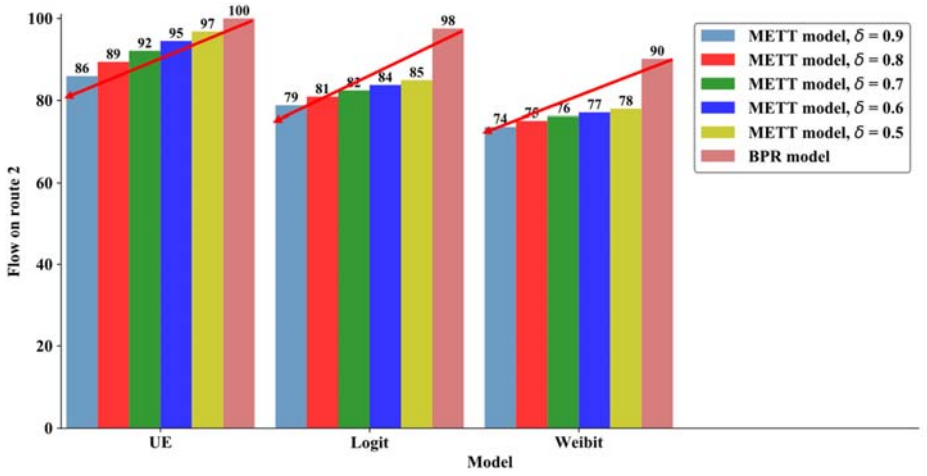

Fig. 8. Flow on route 2 produced by METT models and BPR models ($\theta_a = 0.5$)

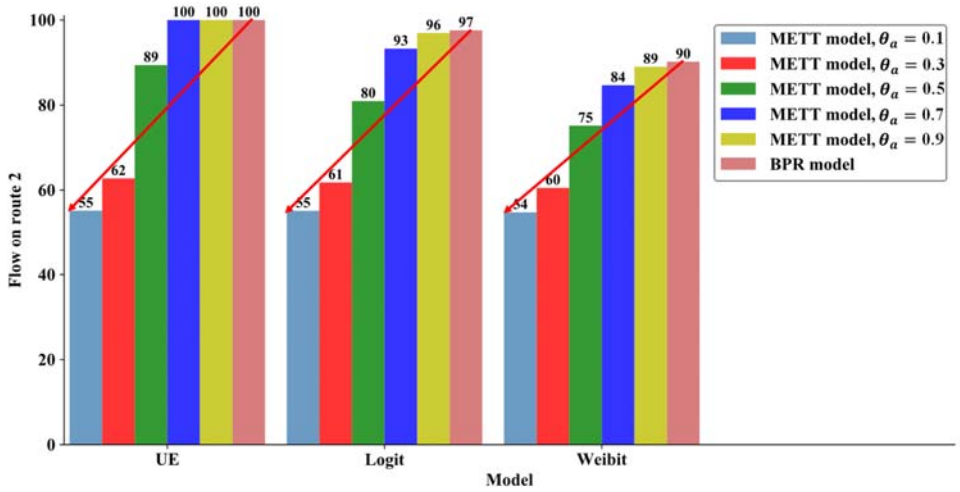

Fig. 9. Flow on route 2 produced by METT models and BPR models ($\delta = 0.8$)

In both figures, the three panels from left to right represent the results from the UE, Logit, and Weibit models, respectively. In Fig. 8, in each of the three panels, as δ increases (i.e., travelers' risk-averseness increases from right to left), the flow difference between the BPR model and the METT model increases. This is because the actual travel time distributions are both with a high peak and a short tail under the given θ_a (See Fig. 7 (a) where $\theta_a = 0.6$, which is close to 0.5 here). Therefore, as δ goes up, the superiority of using the shorter route declines. A similar trend can be observed in Fig. 9. In each of the three categories, as θ_a decreases (i.e., travel time variability induced by link capacity degradation increases from right to left), the flow difference between the BPR model and METT model tends to increase. This is because as θ_a decreases, the variance of the actual travel time increases sharply, and the actual travel time distribution grows to have a low peak and a long tail. When travelers are conservative, (e.g., $\delta = 0.8$ in this case), less of them would use the shorter route (with a smaller mean but a larger variance) as θ_a

decreases. However, it is noticeable that when θ_a equals 0.7 and 0.9, the equilibrium flow patterns of the BPR model and the METT model are the same. This still can be explained by the perfect information assumption in the UE model. That is, when the degree of link capacity degradation is not large enough, the UE-METT model still assumes that all the travelers choose the shorter route. This further illustrates the importance of incorporating subjective uncertainty.

Below we further demonstrate the effect of travel time variability. Since this paper focuses on the Weibit model, we select the Weibit-METT and Weibit models for comparison. Note that Fig. 7(a) has shown the actual travel time distribution of the Weibit-METT model when $\delta = 0.8$ and $\theta_a = 0.6$. We further mark the costs of the two routes at the equilibrium state in the Weibit model and the Weibit-METT model in Fig. 10. At the equilibrium state, the flows on route 1 and 2 are 9.84 and 90.16 respectively in the Weibit model, and 19.27 and 80.73 respectively in the Weibit-METT model. In the Weibit model, BPR function is used to calculate the deterministic travel time without variability. By contrast, the METT in the Weibit-METT model considers both the travel time variability and travelers' attitudes towards risk, as discussed in Section 4.1.1. Although in this case, the costs of route 1 in the Weibit and Weibit-METT models are quite similar (10.01 versus 10.00), there is a larger difference in the costs of route 2 (6.80 versus 5.50). As a result, in the Weibit-METT model, the relative cost difference between the two routes at the equilibrium state is 1.47 (10.01/6.80), which is smaller than 1.82 (10/5.5) in the Weibit model. Hence, less flow is assigned onto the shorter route (route 2) in the Weibit-METT than in the Weibit model. Similar results can also be obtained between the UE-METT and UE models, and between the Logit-METT and Logit models.

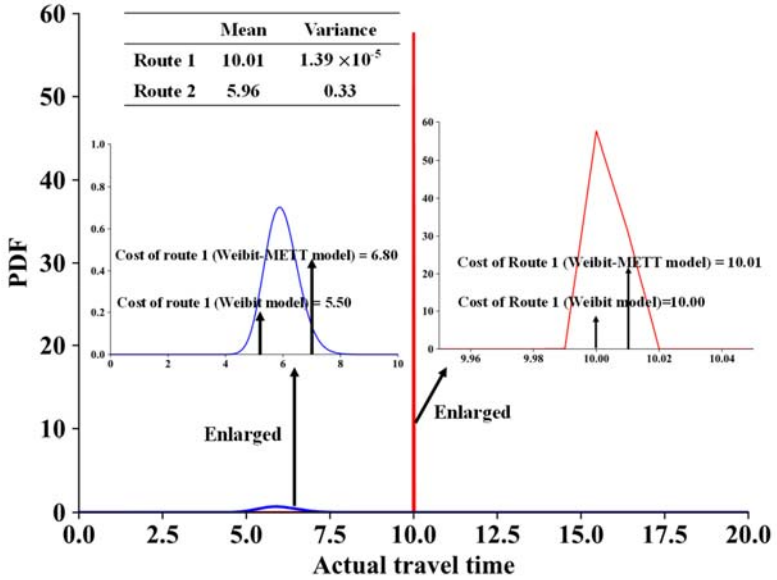

Fig. 10. Actual travel time distributions and equilibrium costs of two routes in the Weibit-METT and Weibit models

From the above analysis, both θ_a and δ can have large impacts on the network flow allocation, especially when the objective uncertainty is high (i.e., small θ_a) or travelers' averseness towards risk is strong (i.e., large δ). The METT day-to-day models are better than the BPR counterparts, because the latter only adopt a deterministic travel time calculated from BPR function to represent the travel cost while ignoring the widely existing travel time variability and travelers' risk-averse attitude. As a result, BPR models tend to overestimate the flow on the shorter route at the equilibrium state. By contrast, METT models use the risk measure of METT to represent travel cost, which captures not only the travel time variability but also travelers' attitudes towards risk. Hence, METT models give rise to more reasonable flow assignment results. In the real world where travelers' risk-averseness towards uncertainty is heterogeneous and the travel time variability widely exists, the METT models are particularly applicable.

4.1.2.2 Comparison among METT models

Section 4.1.2.1 demonstrates the superiority of METT models over BPR models from the perspective of modeling objective uncertainty. Below we focus on the perspective of modeling subjective uncertainty by comparing the proposed Weibit-METT model with the other METT models (i.e., UE-METT and Logit(s)-METT models).

In this example, we use both long and short networks shown in Fig. 3. We still set θ_a to be 0.6 and δ to be 0.8. Besides, we consider two types of Logit models: Logits-METT model (i.e., with scaling) and Logit-METT model (i.e., without scaling). In the Logits-METT model, φ takes different values for the two networks to keep the same CoV with the Weibit-METT model for a fair comparison; and in the Logit-METT model, φ is fixed at 0.1 in both networks.

The results are shown in Table 3. We can see that the UE-METT model assigns more flows on route 2 than the other models in both networks. This phenomenon is even more pronounced in the short network, where the UE-METT model assigns all the demand to route 2, although there is only a slight cost difference between the two routes (10 and 9.29). This again is due to travelers' perfect information and rational behavior assumptions. However, the results of the three SUE-METT models (i.e., Logit-METT, Logits-METT, and Weibit-METT) are also different. The difference between the Weibit-METT and Logit-METT models is larger than that between the Weibit-METT and Logits-METT models. Moreover, the Logit-METT model even assigns less flow onto the shorter route (route 2) than the Weibit-METT model in the short network. The reason is that in the small network, the fixed dispersion parameter φ = 0.1 leads to a much larger CoV in the Logit-METT model than 0.3 in the Weibit-METT model. Note that the difference among three SUE-METT models lies in different assumptions on the perception

variance distributions, which will be further discussed below.

For a fair comparison, we plot the perceived route cost distributions of the Logits-METT model and Weibit-METT model which have the same CoV in both networks in Fig. 11(a) and (b). In both networks, the perceived travel costs of two routes have identical variance in the Logits-METT model. Intuitively, travelers on the longer route (i.e., route 1) should have a larger perception variance, and this is well reflected in the Weibit-METT model. Particularly, the ratio of perception variance between the two routes (route 1/route 2) reaches up to 2.17 in the short network, which is smaller (1.05) in the long network. Also, the Logits-METT model has a smaller perception variance than the Weibit-METT model. These explain why the flow on the longer route produced by the Logits-METT model is underestimated, and why this underestimation is more evident in the short network (as shown in Table 3) where perception errors are smaller and there is a lower opportunity for "wrong" perception in the sense of choosing a longer route. Note that this finding is consistent with Kitthamkesorn and Chen (2013, 2014) where the objective uncertainty was not considered in their Weibit model. Accordingly, the Weibit-METT day-to-day dynamic model can better capture travelers' route choice behavior than the UE-METT or Logits-METT models, because it does not have the perfect information assumption in the UE-METT model or the identically distributed perception error assumption in the Logits-METT model. As for the Logit-METT model, it even assumes a fixed perception variance for the routes in two networks of different lengths, so it is inferior to the Weibit-METT model as well.

Table 3 Results of flows and costs in the two networks

Network		Model			
		UE-METT	Logit-METT (Without scaling, $\varphi = 0.1$)	Logits-METT (With scaling)	Weibit-METT
Short network	Flow on route 1	0	38.71	11.48	19.27
	Flow on route 2	100	61.3	88.52	80.72
	Cost of route 1	10	10.19 (56.75)	10.00 (14.03)	10.01 (3.10)
	Cost of route 2	9.29	5.59 (56.75)	7.61 (14.03)	6.80 (3.10)
Long network	Flow on route 1	44.91	46.32	47.55	47.83
	Flow on route 2	55.09	53.68	52.45	52.17
	Cost of route 1	129.24	129.80 (178.16)	130.33 (266.80)	130.46 (5.92)
	Cost of route 2	129.24	128.33 (178.16)	127.59 (266.80)	127.43 (5.92)

Note: The numbers in the parenthesis are the generalized route costs.

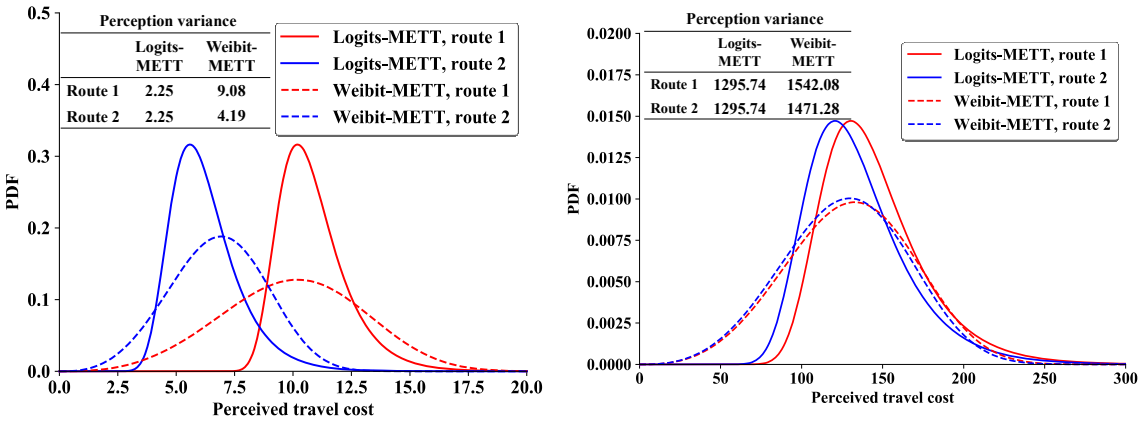

(a) Short network (b) Long network

Fig. 11. Comparison of the perceived cost distributions between the Logits-METT model and Weibit-METT model

The experiments in the two-route networks reveal the advantages and the necessities of the proposed model in characterizing travelers' route choice adjustment behavior. On the one hand, travelers' risk-averseness towards travel time variability can be well captured via the METT concept. On the other hand, the heterogeneous perception variance can be characterized by the Weibit model. Ignoring the objective uncertainty or improperly considering subjective uncertainty can lead to bias in traffic flow assignment, which would further affect the result of vulnerability analysis. By combining the METT concept and the Weibit model, the proposed model provides a new exploration in route choice modeling, which can more comprehensively characterize travelers' route choice behavior. The proposed model lays a foundation for the network vulnerability analysis in terms of the flow evolution prediction, network performance assessment as well as computational tractability.

4.2 Winnipeg Network

In this example, we adopt the Winnipeg network shown in Fig. 12 to demonstrate the property of the proposed method for day-to-day dynamic network vulnerability analysis. The Winnipeg network consists of 154 zones, 1067 nodes, 2535 links, and 4345 O-D pairs. We use a pre-generated route set with 174491 routes. As shown in Fig. 12, there are 14 major bridges as the main crossings of the Red River (eastbound–westbound direction) and the Assiniboine River (northbound–southbound direction) in the downtown and suburban areas.

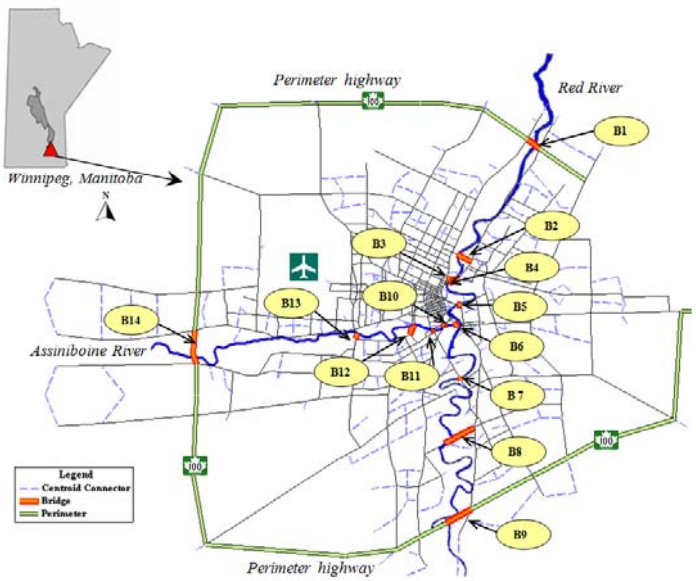

Fig. 12. Winnipeg network and locations of 14 major bridges (Source: Xu *et al*., 2018a).

To examine the generality of the result in Section 4.1.1, we further illustrate the difference among the three day-to-day dynamic models (i.e., UE, Logit and Weibit-METT models) in such a realistic network. The root mean square error (RMSE) of link flow at the equilibrium state is used to measure the difference. The RMSE between models m and n is denoted by $\mathrm{RMSE}^{m,n}$, whose formulation is

$$\mathrm{RMSE}^{m,n} = \sqrt{\sum_{a\in A} \frac{(v_a^m - v_a^n)^2}{|A|}}, \tag{25}$$

where m and n represent different models; and $|A|$ is the number of links in the network. A low value of $\mathrm{RMSE}^{m,n}$ implies that model m performs similarly to model n.

$\mathrm{RMSE}^{\mathrm{UE,Logit}}$, $\mathrm{RMSE}^{\mathrm{UE,Weibit-METT}}$ and $\mathrm{RMSE}^{\mathrm{Logit,Weibit-METT}}$ are 142.75, 196.35, and 106.45, respectively, which means that the difference among the three day-to-day dynamic models is quite pronounced. Besides, at the equilibrium state, the total travel time (TTT) of UE, Logit and Weibit-METT models are 8.12×10^5, 8.99×10^5, and 9.24×10^5, respectively. Obviously, the TTT difference between the UE and Weibit-METT model is the largest, followed by that between the UE and Logit models. This is reasonable because compared to the UE model, the proposed model considers both subjective and objective uncertainties.

Further, the 30-day flow evolution trajectories of link 359 (i.e., westbound of bridge 1) from the three different models are shown in Fig. 13. The flow evolution trajectory resulting from the Weibit-METT model is significantly different from those generated by the other two models. These validate the difference among the three day-to-day models in large-scale networks.

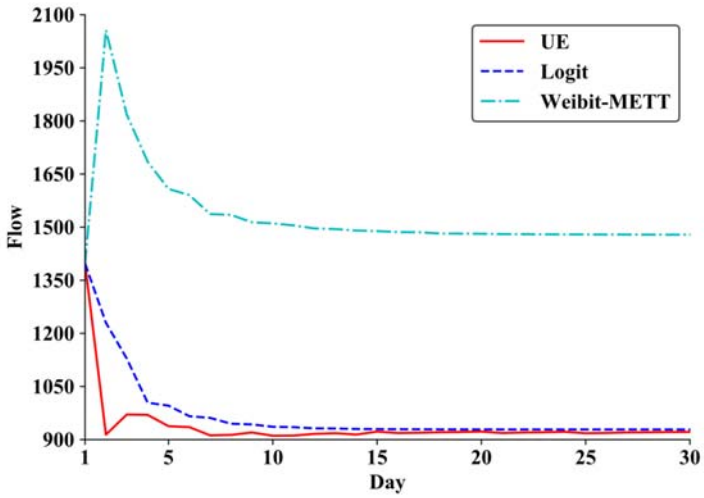

Fig. 13. Flow evolution trajectories of link 359 (westbound of bridge 1) from different models

In the following, 14 disruption scenarios are used to compare the results of vulnerability analysis (i.e., importance rankings of bridges) based on the proposed metric and the traditional metric. In each disruption scenario, one of the 14 bridges is disrupted at both directions. In consistence with the previous example, we still assume θ_a to be 0.6 for all links, and δ to be 0.8. The link travel cost in the Weibit-METT model follows an exponential function (Hensher and Truong, 1985; Mirchandani and Soroush, 1987; Kitthamkesorn and Chen, 2014):

$$\tau_a = e^{0.075\eta_a} \quad \forall a \in A \tag{26}$$

The initial flow pattern is obtained under the same setting as in Section 4.1, and it takes around 30 days to converge. Therefore, we take the TETT on day 30 (i.e., 1.055×10^6) to be the network-wide performance at the pre-disruption equilibrium state. At the end of day 30, we destroy one bridge by setting the free-flow travel time to 999 and compute the two metrics on day 60 (i.e., 30 days after the disruption). Note that the bridge failure is assumed to last throughout the time period after disruption, i.e., from day 30 to day 60.

The importance rankings of the 14 bridges using the two metrics based on the proposed day-to-day dynamic model are presented in Table 4. Fig. 14 illustrates the difference between the proposed metric and the traditional metric under the disruption of bridge 1. The proposed metric is represented by the area (in grey color) circled by the post-disruption TETT curve in the grape solid line and the pre-disruption TETT at the equilibrium in the blue dashed line. By contrast, the traditional metric is only represented by a single point of the TETT at the final equilibrium state (i.e., TETT on day 60). Intuitively, the traditional metric only concerns the performance at the final state, ignoring the evolution of system performance after the disruption. In Fig. 14, after the disruption of bridge 1, TETT surges to the peak of 2.971×10^6 one day later, recovers to 1.05 times of the TETT at the original equilibrium state 13 days after the disruption, and then converges to 1.086×10^6 on day 60. It is worth mentioning that the peak value of TETT after the disruption of bridge 1 is nearly 3 times that of the final state. Using only the final state may

significantly underestimate the cumulative impact of the bridge disruption.

Table 4. The value of the two metrics and corresponding rankings of 14 bridges

Bridge	The proposed metric ($\times 10^6$)	Traditional metric ($\times 10^6$)	Ranking based on the proposed metric (R^p)	Ranking based on the traditional metric (R^t)
Bridge 1	5.169	1.086	8	3
Bridge 2	3.546	1.057	11	12
Bridge 3	3.384	1.055	13	14
Bridge 4	7.490	1.078	6	4
Bridge 5	7.751	1.072	5	6
Bridge 6	9.821	1.086	3	2
Bridge 7	5.032	1.0627	9	10
Bridge 8	4.127	1.059	10	11
Bridge 9	1.366	1.056	14	13
Bridge 10	10.464	1.075	2	5
Bridge 11	8.707	1.0629	4	9
Bridge 12	5.180	1.071	7	7
Bridge 13	15.368	1.124	1	1
Bridge 14	3.502	1.070	12	8

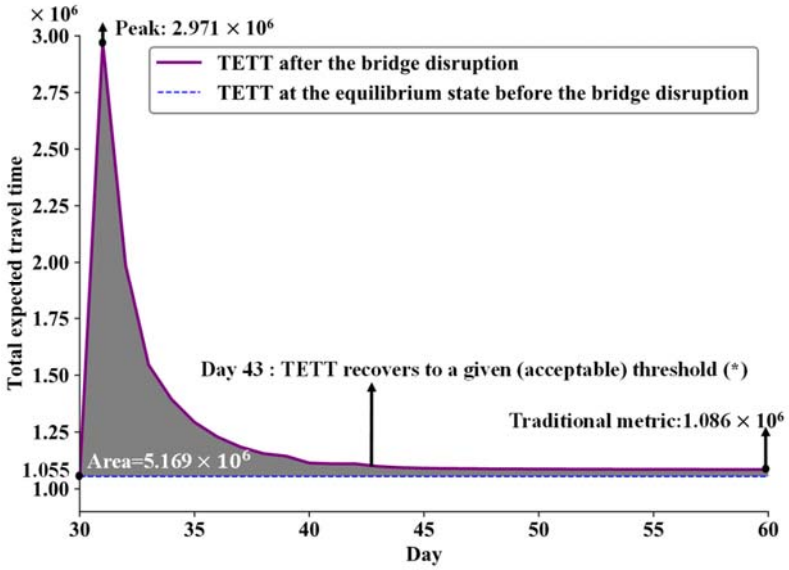

Note:(*): TETT recovers to 1.05 times of that at the original equilibrium state 13 days after the disruption

Fig. 14. Illustrations of the proposed and traditional metrics under the disruption of bridge 1

Similar to the traditional metric, the proposed metric DNP is still a scalar. In engineering practice, it is easier and more intuitive for managers to distinguish the relative importance of network components by comparing a scalar value than comparing groups of multiple numbers or probability distributions. Despite being a scalar, the proposed metric essentially integrates multiple aspects of the post-disruption network performance fluctuation. Specifically, the

proposed metric has three important elements, i.e., performance peak, number of days required to recover to an acceptable threshold, and network performance at the final state. The metric DNP is an accumulated metric, which is the integration of TETT over multiple days. Thus, in most cases, different disruption scenarios tend to generate different DNP values. However, it is theoretically possible to encounter the same value of the proposed metric under different disruption scenarios, and we can use the three abovementioned important elements as the secondary metrics to distinguish such scenarios. The three important elements under different bridge disruption scenarios are provided in Table 5.

Table 5 Key factors on the evolution of TETT under different disruption scenarios

Bridge	The peak of TETT ($\times 10^6$)	TETT on day 60 ($\times 10^5$)	The ratio of the TETT peak to TETT on day 60	Days required to recover to a given threshold (*)
Bridge 1	2.971	1.086	2.737	13
Bridge 2	2.949	1.057	2.791	8
Bridge 3	2.654	1.055	2.515	8
Bridge 4	4.688	1.078	4.346	13
Bridge 5	5.353	1.072	4.993	10
Bridge 6	5.847	1.086	5.384	13
Bridge 7	3.450	1.0627	3.247	10
Bridge 8	3.012	1.059	2.843	8
Bridge 9	1.648	1.056	1.560	5
Bridge 10	7.287	1.075	6.781	11
Bridge 11	6.605	1.0629	6.215	10
Bridge 12	3.279	1.071	3.063	11
Bridge 13	7.988	1.124	7.109	Cannot recover within 30 days
Bridge 14	2.383	1.070	2.227	9

Note: (*) denotes the days required for TETT to recover to 1.05 times of that at the pre-disruption equilibrium state

To provide a more intuitive understanding, the rankings of bridges based on the two metrics are demonstrated in Fig. 15. It is obvious that except for two bridges (i.e., bridges 12 and 13), all the remaining 12 bridges are ranked differently using the two metrics. Seven bridges (i.e., bridges 2, 3, 5, 7, 8, 10, 11) are ranked higher based on the proposed metric, while five bridges (bridges 1, 4, 6, 9, 14) are deemed to be more important by the traditional metric. Further, we use the metric r-square, which can reflect how well the dataset of rankings are fitted to the 45° line (i.e., the line $R^t = R^p$), to evaluate how large the difference between the rankings is. Note that r-square is usually used to evaluate the goodness of fit in statistics, which takes the value ranging from 0 to 1, with a larger value indicating a higher goodness of fit (Cohen, 1988). In Fig.15, the r-square is 0.622, implying a relatively large difference between the ranking results under the two metrics. Due to such a large difference between the ranking results and considering that the proposed metric integrates multiple aspects of the post-disruption network performance fluctuation rather than merely focusing on the final state as in the traditional metric, it is meaningful to use the proposed metric for critical network components identification.

Besides, it is notable from Fig. 15 that, bridges 1 and 11 deviate the most from the 45° line, both with an absolute ranking difference of 5 under the two metrics. For a further discussion, the evolution trajectories of TETT under the two scenarios are plotted in Fig. 16.

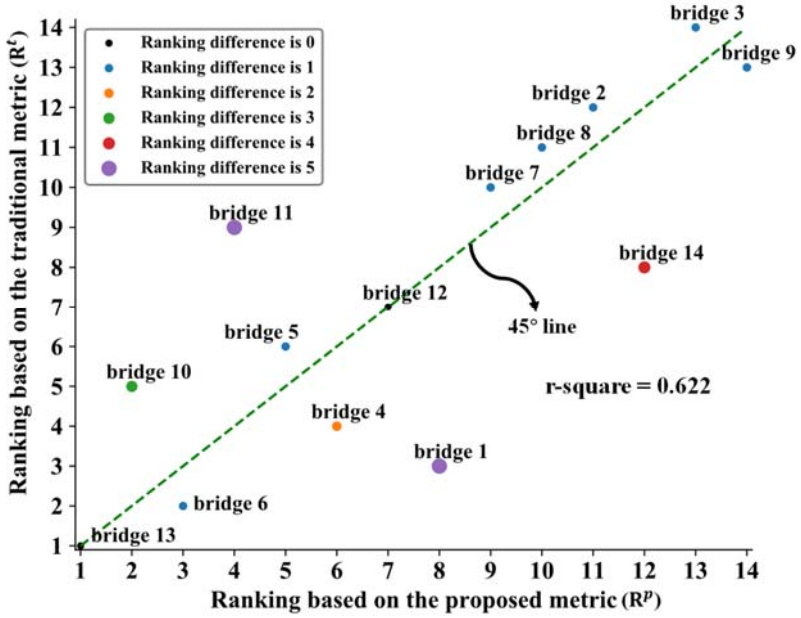

Fig. 15 Rankings of bridges based on two metrics

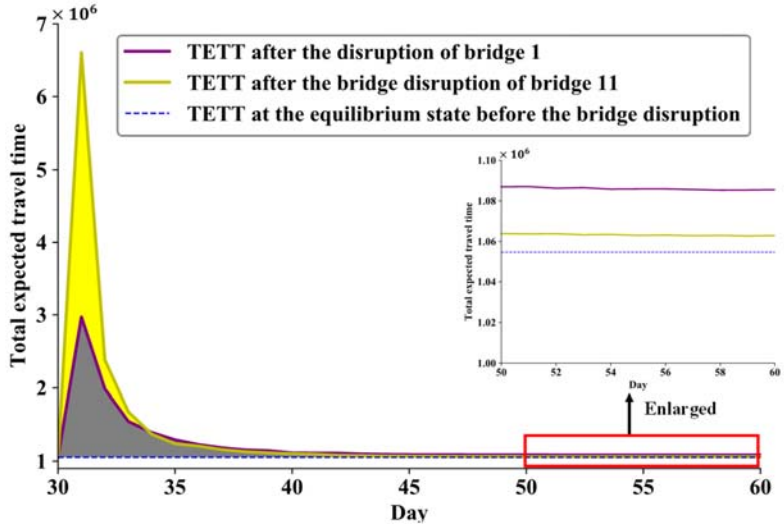

Fig. 16 Comparison of the TETT evolution trajectories under the disruptions of bridge 1 and 11

Fig. 16 together with Tables 4 and 5 can well explain the large ranking difference of the two bridges using the two metrics. For bridge 1, although the value of the traditional metric at the final state is relatively large and ranks the 3rd, the disruption impact over the whole evolution process is not so significant due to its relatively low peak and short recovery time. As a result, the traditional metric largely overestimates the importance of bridge 1. Regarding bridge 11,

despite the traditional metric at the final state is relatively small and ranks the 9th only, its cumulative impact over the whole evolution process is much larger primarily owing to the significantly high peak. Hence, the traditional metric largely underestimates the importance of bridge 11.

Besides, the range of the proposed metric is much larger than that of the traditional metric. More specifically, in the second column of Table 4, the largest value is 1.537×10^7 of bridge 13, which is more than 10 times that of the least important bridge (1.366×10^6 of bridge 9). Even for the two most important bridges (i.e., bridge 13 and 10), their difference based on the proposed metric is around 1.5 times. This can be explained by Table 5. After the disruption of bridge 13, the TETT even cannot recover to 1.05 times of the pre-disruption equilibrium state. By contrast, based on the traditional metric, the largest relative difference between the most important bridge and the least important bridge is only 1.06 times (i.e., 1.124×10^6 of bridge 13 versus 1.055×10^6 of bridge 3). Obviously, the difference among the bridges is much less evident based on the traditional metric. The results based on the proposed metric deliver a message to transportation managers that bridge 13 should be given a much higher priority to than the other bridges, but the results based on the traditional metric fail to indicate such a large gap in the relative importance among bridges. What's more, it is difficult to distinguish the relative importance of bridges 7 and 11 based on the traditional metric (1.0627×10^6 versus 1.0629×10^6), while the disruptions of the two bridges lead to quite different peak values of network performance (5.032×10^6 versus 8.707×10^6) as revealed in the proposed metric. From this perspective, the proposed metric has a better capability to distinguish the importance of critical components than the traditional metric. Note that all the above analyses are based on the discrete day-to-day dynamic model. The bridge importance rankings based on the continuous day-to-day model are also provided in Appendix E for a comparison.

To sum up, the proposed metric outperforms the traditional metric in two aspects. First, the traditional metric only pays attention to the final state and ignores the network performance evolution after the disruption, which is likely to lead to a biased result of vulnerability analysis. The worst performance (i.e., the peak) after the disruption could be very severe relative to the final equilibrium state. With the day-dependent network performance information, planners and managers can determine the recovery strategy if needed. Besides, the proposed metric is more sensitive to different disruptions scenarios, and hence has a better capability of distinguishing the importance of different network components than the traditional metric.

5 CONCLUDING REMARKS

The disruptions encountered in the transportation network vulnerability analysis are generally associated with severe infrastructure damages and last for a long time period (from weeks to months) before the complete recovery. This would inevitably affect travelers' day-to-day route choice behaviors and result in day-to-day network performance fluctuation. In this paper, we develop a new day-to-day dynamic network vulnerability analysis approach that allows the consideration of day-to-day network performance fluctuation based on a new day-to-day model under both objective and subjective uncertainties. Compared to most existing day-to-day models that either adopt UE or Logit-based route choice criterion, the advantages of the new day-to-day model are twofold: firstly, the Weibit model is used to capture travelers' subjective perception error uncertainty, which overcomes the drawback of the UE model due to the perfect information assumption, and the drawback of the Logit model due to the identically distributed perception error assumption; secondly, the METT concept is used to capture the objective travel time uncertainty, which overcomes the deficiency of ignoring travel time variability in most existing day-to-day models while remaining computational tractability, making it applicable to vulnerability analysis in large-scale networks. Based on the proposed day-to-day dynamic model, we develop a new component importance metric. The new metric characterizes the post-disruption day-dependent consequences to alleviate the limitation of only assessing the final static equilibrium consequence as in the existing studies of vulnerability analysis.

Numerical examples are conducted to demonstrate the superiority of the proposed day-to-day dynamic model and the new component importance metric, as well as their applicability in large-scale networks. More specifically, we show that (1) improper consideration or ignorance of subjective uncertainty and/or objective uncertainty in the commonly used static UE and Logit models may lead to biased results of flow assignment, which can further influence the vulnerability analysis result; (2) compared to the traditional metric which only focuses on the equilibrium state, the new metric not only considers the performance evolution after the disruption but also has a better capability of distinguishing the importance of different network components. By introducing the day-to-day time dimension into the vulnerability analysis, the proposed method provides a new decision support tool for planners and managers with the following multiple functions: (1) identifying the critical network components and planning for system protection against disruptions; (2) determining the threshold of activating the recovery schedule, i.e., whether and when to start the recovery schedule after disruption; and (3) evaluating the performance of network strengthening or improvement plans.

A few directions are worthy of further investigations: (1) Although the Weibit model can handle the issue of the identically distributed perception error assumption of the Logit model, it still inherits the independently distributed perception error assumption. We can easily extend the proposed model to further consider the route overlapping issue by introducing the path-size factor. (2) Empirical analyses are necessary to validate our model as well as the rationality of the flow adjustment strategy. (3) This paper adopts the TETT as the performance measure in the vulnerability analysis. It would also be interesting to investigate the application of other performance measures, e.g., accessibility and redundancy. (4) In addition to the link disruption consequence, we can further consider the link disruption probability in vulnerability analysis with the increasing data availability (e.g., Esfeh *et al*., 2020). (5) We can adopt a more general or a more travel behavior-oriented day-to-day model to better characterize travelers' behavior, e.g., the Bayesian day-to-day model recently proposed by Zhu et al. (2019) to relax the assumptions on supply distribution, and even the route choice criterion.

APPENDIX A

As introduced in Eq. (7), we adopt the BPR link performance function. For the case of uniformly distributed link capacity uncertainty, the mean and variance of link travel time have been derived in Lo *et al*. (2006). Assume the upper bound and the lower bound of the link capacity are respectively $\bar{c}_a$ and $\theta_a \bar{c}_a$. Then the formulas of the mean and variance of link travel time are as follows:

$$E(T_a) = t_a^0 + \gamma t_a^0 v_a^b \frac{(1-\theta_a^{1-b})}{\bar{c}_a^b (1-\theta_a)(1-b)} \tag{A.1}$$

$$var(T_a) = \gamma^2 (t_a^0)^2 v_a^{2b} \{\frac{1-\theta_a^{1-2b}}{\bar{c}_a^{2b}(1-\theta_a)(1-2b)} - [\frac{1-\theta_a^{1-b}}{\bar{c}_a^{\beta}(1-\theta_a)(1-b)}]^2\} \tag{A.2}$$

We use lognormal distribution to characterize link travel time variability, i.e., $T_a \sim \mathrm{LN}(\mu_{a,t}, \sigma_{a,t})$, and its two parameters can be inversely calculated as follows:

$$\mu_{a,t} = \ln\big(E(T_a)\big) - \frac{1}{2}\ln(1 + \frac{var(T_a)}{[E(T_a)]^2}) \tag{A.3}$$

$$\sigma_{a,t}^2 = \ln(1 + \frac{var(T_a)}{[E(T_a)]^2}) \tag{A.4}$$

Based on the two parameters (i.e., $\mu_{a,t}$ and $\sigma_{a,t}$), the PDF of link travel time has been known. Then, following Xu *et al*. (2017), the calculation formula of link METT can be obtained.

APPENDIX B

We first show that the RTFA can be derived by partially linearizing the objective function $\mathrm{Z}(\mathbf{f})$ in Eq. (15). For ease of demonstration, we denote the first term in Eq. (15) (i.e.,

$\sum_{a\in A}\int_0^{\sum_{w\in W}\sum_{r\in R^w} f_{w,r}\rho_{ra}^w} \ln\tau_a(w)dw$) as $\mathrm{W}(\mathbf{f})$, and the second term (i.e., $\sum_{w\in W}\frac{1}{\beta^w}\sum_{r\in R^w} f_{w,r}(\ln f_{w,r}-1)$) as $\mathrm{G}(\mathbf{f})$.

By using a first-order approximation to the first term of Eq. (15), we can obtain the following partial linearization subproblem

[Partial-L]

$$\min_{\mathbf{f}\in\Omega} \nabla_{\mathbf{f}}\mathrm{W}(\mathbf{f}^{(k)})^T(\mathbf{f}-\mathbf{f}^{(k)}) + \mathrm{G}(\mathbf{f}) \tag{B.1}$$

Eq. (B.1) can be rewritten as follows

$$\min_{\mathbf{f}\in\Omega} \sum_{w\in W}\sum_{r\in R^w} \ln g_{w,r}^{(k)}\cdot f_{w,r} + \sum_{w\in W}\frac{1}{\beta^w}\sum_{r\in R^w} f_{w,r}\cdot(\ln f_{w,r}-1) \tag{B.2}$$

It can be seen that Eq. (B.2) is exactly the RTFA.

We now prove Proposition 1 next. It can be easily seen that the model Partial-L has at least one optimal solution because it is a convex program with a non-empty feasible solution set. By Theorem 3.4.3 in Bazaraa *et al*. (2006), if $\mathbf{f}^{(k)}$ is a minimizer to Partial-L, we have the following variational inequality (VI):

$$[\nabla_{\mathbf{f}}\mathrm{W}\left(\mathbf{f}^{(k)}\right)^T + \nabla\mathrm{G}(\mathbf{f}^{(k)})](\mathbf{f}-\mathbf{f}^{(k)}) \geq 0 \tag{B.3}$$

By simple calculations, one can easily verified that Eq. (B.3) is equivalent to the VI formulation of the Weibit-based SUE. Therefore, $\mathbf{f}^{(k)}$ is the route flow pattern of the Weibit-based SUE.

If $\mathbf{f}^{(k)}$ does not solve Partial-L, since $\mathbf{y}^{(k)}$ is a solution to this problem, then

$$\nabla_{\mathbf{f}}\mathrm{W}\left(\mathbf{f}^{(k)}\right)^T\left(\mathbf{y}^{(k)}-\mathbf{f}^{(k)}\right) + \mathrm{G}\left(\mathbf{y}^{(k)}\right) < \nabla_{\mathbf{f}}\mathrm{W}\left(\mathbf{f}^{(k)}\right)^T\left(\mathbf{f}^{(k)}-\mathbf{f}^{(k)}\right) + \mathrm{G}\left(\mathbf{f}^{(k)}\right) = \mathrm{G}\left(\mathbf{f}^{(k)}\right) \tag{B.4}$$

By the convexity of $\mathrm{G}(\cdot)$, we have

$$\mathrm{G}\left(\mathbf{y}^{(k)}\right) - \mathrm{G}\left(\mathbf{f}^{(k)}\right) \geq \nabla\mathrm{G}\left(\mathbf{f}^{(k)}\right)\left(\mathbf{y}^{(k)}-\mathbf{f}^{(k)}\right) \tag{B.5}$$

Combining Eqs. (B.4) and (B.5), we have

$$\left[\nabla_{\mathbf{f}}\mathrm{W}\left(\mathbf{f}^{(k)}\right)^T + \nabla\mathrm{G}(\mathbf{f}^{(k)})\right]\left(\mathbf{y}^{(k)}-\mathbf{f}^{(k)}\right) < 0 \tag{B.6}$$

which is equivalent to

$$\left[\ln\mathbf{g} + \frac{1}{\beta^w}\ln\mathbf{f}\right]\left(\mathbf{y}^{(k)}-\mathbf{f}^{(k)}\right) < 0 \tag{B.7}$$

where $\ln\mathbf{g} + \frac{1}{\beta^w}\ln\mathbf{f}$ is the generalized cost ($\tilde{\mathbf{g}}\left(\mathbf{f}^{(k)}\right)$) in the Weibit-SUE model. Substituting Eq. (1) into Eq. (B.7), we have

$$\tilde{\mathbf{g}}\left(\mathbf{f}^{(k)}\right)^{\mathrm{T}}\left(\mathbf{f}^{(k+1)}-\mathbf{f}^{(k)}\right) < 0 \tag{B.8}$$

which is the desired result of Proposition 1.

APPENDIX C

It is obvious that when $\mathbf{y}^{(k)} - \mathbf{f}^{(k)} = 0$, i.e., the convergence is reached, Eq. (21) holds. For the case that $\mathbf{y}^{(k)} \neq \mathbf{f}^{(k)}$, consider a function

$$Z\left(\alpha^{(k)}\right) = Z\left(\left(1-\alpha^{(k)}\right)\mathbf{f}^{(k)} + \alpha^{(k)}\mathbf{y}^{(k)}\right) = Z(\mathbf{f}^{(k+1)}) \tag{C.1}$$

We have the following first-order derivative

$$\frac{dZ\left(\alpha^{(k)}\right)}{d\alpha^{(k)}} = \left(\frac{\partial Z(\mathbf{f}^{(k+1)})}{\partial \mathbf{f}^{(k+1)}}\right)^T \frac{d\mathbf{f}^{(k+1)}}{d\alpha^{(k)}} = \tilde{\mathbf{g}}\left(\left(1-\alpha^{(k)}\right)\mathbf{f}^{(k)} + \alpha^{(k)}\mathbf{y}^{(k)}\right)^T \left(\mathbf{y}^{(k)} - \mathbf{f}^{(k)}\right)$$

When $\alpha^{(k)} = 0$, combining Eq. (B.5), we have

$$\left.\frac{dZ\left(\alpha^{(k)}\right)}{d\alpha^{(k)}}\right|_{\alpha^{(k)}=0} = \tilde{\mathbf{g}}\left(\mathbf{f}^{(k)}\right)^T\left(\mathbf{y}^{(k)} - \mathbf{f}^{(k)}\right) < 0 \tag{C.2}$$

The derivative of the generalized cost $\tilde{\mathbf{g}}(\mathbf{f}^{(k)})$ with respect to route flow is,

$$\frac{\partial \tilde{\mathbf{g}}(\mathbf{f}^{(k)})}{\partial \mathbf{f}^{(k)}} = \frac{1}{\mathbf{f}^{(k)}}$$

Since route flow $\mathbf{f}^{(k)}$ is non-negative, $\frac{\partial \tilde{\mathbf{g}}(\mathbf{f}^{(k)})}{\partial \mathbf{f}^{(k)}} > 0$.

Then we have

$$\frac{d^2 Z\left(\alpha^{(k)}\right)}{d{\alpha^{(k)}}^2} = \left(\mathbf{y}^{(k)} - \mathbf{f}^{(k)}\right)^T \frac{1}{\mathbf{f}^{(k)}}\left(\mathbf{y}^{(k)} - \mathbf{f}^{(k)}\right) > 0 \tag{C.3}$$

Furthermore, function $Z\left(\alpha^{(k)}\right)$ is strictly convex when $\alpha^{(k)} \in [0,1]$. It follows from Eqs. (C.2) and (C.3) that there is $\overline{\alpha^{(k)}} \in (0,1]$ so that

$$\frac{dZ\left(\alpha^{(k)}\right)}{d\alpha^{(k)}} = \tilde{\mathbf{g}}\left(\left(1-\alpha^{(k)}\right)\mathbf{f}^{(k)} + \alpha^{(k)}\mathbf{y}^{(k)}\right)^T\left(\mathbf{y}^{(k)} - \mathbf{f}^{(k)}\right) \leq 0, \qquad \forall \alpha^{(k)} \in \left(0, \overline{\alpha^{(k)}}\right]$$

Therefore, $Z(0) > Z\left(\alpha^{(k)}\right)$. Recall from (C.1) that $Z(0) = Z(\mathbf{f}^{(k)})$ and $Z\left(\alpha^{(k)}\right) = Z(\mathbf{f}^{(k+1)})$. So, we have $Z\left(\mathbf{f}^{(k)}\right) > Z(\mathbf{f}^{(k+1)})$. This means that as days go on, when $\mathbf{y}^{(k)} \neq \mathbf{f}^{(k)}$, namely when the target flow on day k+1 is not equal to the route flow on day k, the objective function will always decrease until $\mathbf{y}^{(k)} = \mathbf{f}^{(k)}$, namely the convergence is reached. Also, recall that the route flow $\mathbf{f}^{(k)}$ that minimizes $Z\left(\mathbf{f}^{(k)}\right)$ satisfies the Weibit-SUE state. Thus, the proposed day-to-day dynamic model evolves towards the Weibit-SUE state under the flow adjustment strategy.

Below we present how to calculate the flow adjustment ratio with the bisection method. The interpretation is as follows. First, let $\alpha^{(k)} = 1$; if Eq. (21) does not hold, then we take $\alpha^{(k)} \leftarrow \alpha^{(k)}/2$ until Eq. (21) holds. According to Proposition 2, $\alpha^{(k)}$ can be deemed an upper bound,

and all the values within the interval (0, $\alpha^{(k)}$] satisfy Eq. (21). Therefore, any value within the interval (0, $\alpha^{(k)}$] can be used as the flow adjustment ratio to guarantee the global convergence of the flow adjustment process. Note that the interval obtained in this manner is most likely to be the subset of the actual interval because the upper bound obtained here is very likely to be smaller than the actual upper bound $\overline{\alpha^{(k)}}$, (i.e., $\alpha^{(k)} \leq \overline{\alpha^{(k)}}$, so the range of (0, $\alpha^{(k)}$] is no larger than that of (0, $\overline{\alpha^{(k)}}$]), and we can take $\alpha^{(k)}$ as the flow adjustment ratio.

Step 1. Let $\alpha^{(k)} = 1$.

Step 2. Calculate $\tilde{\mathbf{g}}\left(\left(1-\alpha^{(k)}\mathbf{f}^{(k)}\right)+\alpha^{(k)}\mathbf{y}^{(k)}\right)^{T}\left(\mathbf{y}^{(k)}-\mathbf{f}^{(k)}\right)$.

Step 3. Check whether $\tilde{\mathbf{g}}\left((1-\alpha^{(k)})\mathbf{f}^{(k)}+\alpha^{(k)}\mathbf{y}^{(k)}\right)^{T}\left(\mathbf{y}^{(k)}-\mathbf{f}^{(k)}\right) \leq 0$. If yes, go to step 4; or else, let $\alpha^{(k)}=\frac{\alpha^{(k)}}{2}$ and go to step 2.

Step 4. Output $\alpha^{(k)}$.

APPENDIX D

Table D.1 Notations and explanations

Notation	Explanation
k	The day index
N	The set of nodes
A	The set of links
W	The set of origin-destination (O-D) pairs
R^w	The set of paths between an O-D pair $w \in W$
$\alpha^{(k)}$	The flow adjustment ratio on day k
$\mathbf{f}^{(k)}$	The column vector of all the path flows on day k, $\mathbf{f}^{(k)} = (f_{w,r}^{(k)},\ r \in R^w, w \in \mathrm{W})^T$
$f_{w,r}^{(k)}$	The traffic flow on path $r \in R^w$ between O-D pair $w \in W$ on day k
$\mathbf{y}^{(k)}$	The column vector of all the target path flows on day k, $\mathbf{y}^{(k)} = (y_{w,r}^{(k)},\ r \in R^w, w \in W)^T$
$y_{w,r}^{(k)}$	The target traffic flow on path $r \in R^w$ between O-D pair $w \in W$ on day k
q^w	The travel demand between $w \in \mathrm{W}$
$v_a^{(k)}$	The flow on link $a \in A$ on day k
ρ_{ra}^w	$\delta_{ra}^w = 1$ if path $r \in R^w$ contains link a, and $\delta_{ar}^w = 0$ otherwise
T_a	The travel time function of link $a \in A$
t_a^0	Free flow travel time of link a
C_a	The capacity of link a
γ	BPR parameter, usually specified as 0.15
b	BPR parameter, usually specified as 4
θ_a	Lower bound of link capacity degradation of link a
β^w	The shape parameter of O-D pair w in the Weibit model
φ	The dispersion parameter in the Logit model

$P_{w,r}^{(k)}$	The probability of choosing route r connecting O-D pair w on day k
$g_{w,r}^{(k)}$	The travel cost of route r between O-D pair w on day k
$\eta_a(\delta)$	The METT of link a at the confidence level of δ
$\xi_a(\delta)$	Travel time budget of link a that satisfies δ-reliability requirement
$\epsilon_a(\delta)$	Buffer time of link a that satisfies δ-reliability requirement
$\sigma_{w,r}$	The perception variance of route r connecting O-D pair w
τ_a	The link travel cost on link a

APPENDIX E

The counterpart continuous-time day-to-day dynamic model is formulated as

$$\dot{\mathbf{f}} = \hat{\alpha}\,(\Phi(\mathbf{g}) - \mathbf{f}), \hat{\alpha} > 0 \tag{E.1}$$

where $\Phi(\mathbf{g}) = (q_w \frac{(g_{w,r})^{-\beta^w}}{\sum_{p\in R^w}(g_{w,p})^{-\beta^w}}, w \in W, r \in R)^T$ is the Weibit loading functions, $\hat{\alpha}$ is the flow adjustment parameter, $\mathbf{g}$ is the path cost vector, and $\mathbf{f}$ is the path flow vector. The continuous day-to-day model is similar to the one in Ye et al. (2021) with travelers taking ATIS information as their perception (since we do not consider the learning process) and ATIS publishing the actual travel time, except that here $\Phi(\cdot)$ is the Weibit loading instead of the Logit loading function. Thus, the convergence property can be proved in a similar fashion as in Ye et al. (2021).

Combining Eqs. (22), (24) and (E.1), the vulnerability analysis based on the continuous day-to-day model can be conducted. The comparison of bridge importance rankings under discrete-time and continuous-time day-to-day models is shown in Table E.1. The vulnerability analysis results under different models are only slightly different. Specifically, among the 14 bridges, the largest ranking difference is no larger than 2. The MSE (mean square error) values between the vulnerability analysis result under the discrete-time model and those under the five continuous-time models are respectively 1, 1, 1, 1.29, and 1.29. In addition, under the six investigated day-to-day models, the most and the least important bridges (i.e., Bridge 13 and Bridge 9 respectively) are the same. The above results indicate that the version of day-to-day models does not have significant influence on the vulnerability analysis results.

Table E.6 Comparison of bridge importance rankings under discrete-time and continuous-time day-to-day models

Bridges	Discrete-time model	Continuous-time models				
		$\hat{\alpha} = 0.1$	$\hat{\alpha} = 0.3$	$\hat{\alpha} = 0.5$	$\hat{\alpha} = 0.7$	$\hat{\alpha} = 0.9$
Bridge 1	8	9	9	8	7	7
Bridge 2	11	12	13	13	13	13
Bridge 3	13	11	11	12	12	12
Bridge 4	6	6	5	4	4	4
Bridge 5	5	5	6	6	5	5
Bridge 6	3	2	2	2	2	2
Bridge 7	9	7	8	9	9	9
Bridge 8	10	10	10	10	10	10
Bridge 9	**14**	**14**	**14**	**14**	**14**	**14**
Bridge 10	2	3	3	3	3	3
Bridge 11	4	4	4	5	6	6
Bridge 12	7	8	7	7	8	8
Bridge 13	**1**	**1**	**1**	**1**	**1**	**1**
Bridge 14	12	13	12	11	11	11

REFERENCES

Abdel-Aty, M.A., Kitamura, R., Jovanis, P.P., 1995. Exploring route choice behavior using geographic information system-based alternative routes and hypothetical travel time information input. *Transportation Research Record* 1493, 74-80.

Bababeik, M., Khademi, N., Chen, A., 2018. Increasing the resilience level of a vulnerable rail network: The strategy of location and allocation of emergency relief trains. *Transportation Research Part E* 119, 110-128.

Bazaraa, M.S., Sherali, H.D., Shetty, C.M., 2006. Nonlinear programming: theory and algorithms. Wiley, New York.

Beckmann, M.J., McGuire, C.B., Winsten, C.B., 1956. *Studies in the economics of transportation*. Yale University press, New Haven, Connecticut.

Bell, M.G.H., Kurauchi, F., Perera, S., Wong, W., 2017. Investigating transport network vulnerability by capacity weighted spectral analysis. *Transportation Research Part B* 99, 251-266.

Berdica, K., 2002. An introduction to road vulnerability: what has been done, is done and should be done. *Transport Policy* 9 (2), 117-127.

Bifulco, G.N., Cantarella, G.E., Simonelli, F.,Velona, P., 2016. Advanced traveller information systems under recurrent traffic conditions: Network equilibrium and stability. *Transportation Research Part B* 92, 73-87.

Calatayud, A., Mangan, J., Palacin, R., 2017. Vulnerability of international freight flows to shipping network disruptions: A multiplex network perspective. *Transportation Research Part E* 108, 195-208.

Cantarella, G.E., Watling, D.P., 2016. A general stochastic process for day-to-day dynamic traffic assignment: Formulation, asymptotic behaviour, and stability analysis. *Transportation Research Part B* 92, 3-21.

Cascetta, E., 1989. A Stochastic-process approach to the analysis of temporal dynamics in transportation networks. *Transportation Research Part B* 23 (1), 1-17.

Castillo, E., Menendez, J.M., Jimenez, P., Rivas, A., 2008. Closed form expressions for choice probabilities in the Weibull case. *Transportation Research Part B* 42 (4), 373-380.

Cats, O., Jenelius, E., 2014. Dynamic vulnerability analysis of public transport networks: mitigation effects of real-time information. *Networks & Spatial Economics* 14 (3-4), 435-463.

Chen, A., Yang, C., 2004. Stochastic transportation network design problem with spatial equity constraint. *Journal of the Transportation Research Board* 1882, 97-104.

Chen, A., Kongsomsaksakul, S., Zhou, Z., Lee, M., Recker, W., 2007a. Assessing network vulnerability

of degradable transportation systems: An accessibility-based approach. *In Proceedings of the 17th International Symposium of Transportation and Traffic Theory*, Elsevier. Edited by M.G.H. Bell, B. Heydecker, and R. Allsop, pp. 236-262.

Chen, A., Yang, C., Kongsomsaksakul, S., Lee, M., 2007b. Network-based accessibility measures for vulnerability analysis of degradable transportation networks. *Network and Spatial Economics* 7 (3), 241-256.

Chen, A., Zhou, Z., 2010. The alpha-reliable mean-excess traffic equilibrium model with stochastic travel times. *Transportation Research Part B* 44 (4), 493-513.

Chen, B.Y., Lam, W.H.K., Sumalee, A., Li, Q.Q., Li, Z.C., 2012. Vulnerability analysis for large-scale and congested road networks with demand uncertainty. *Transportation Research Part A* 46 (3), 501-516.

Chen, B.Y., Lam, W.H.K., Sumalee, A., Li, Q.Q., Tam, M.L., 2014. Reliable shortest path problems in stochastic time-dependent networks. *Journal of Intelligent Transportation Systems* 18 (2), 177-189.

Cheng, Q.X., Wang, S.A., Liu, Z.Y., Yuan, Y., 2019. Surrogate-based simulation optimization approach for day-to-day dynamics model calibration with real data. *Transportation Research Part C* 105, 422-438.

Cohen, J., 1988. Statistical power analysis for the behavioral sciences, second ed. Lawrence Erlbaum Associates, Hillsdale, New Jersey.

Daganzo, C.F., Sheffi, Y., 1977. On stochastic modes of traffic assignment. *Transportation Science* 11 (3), 253-274.

D'Este, G.M., Taylor, M.A.P., 2003. Network vulnerability: An approach to reliability analysis at the level of national strategic transport networks. *Proceedings of the 1st International Symposium on Transportation Network Reliability* (*INSTR*).

Dial, R.B., 1971. A probabilistic multipath traffic assignment model which obviates path enumeration. *Transportation Research* 5 (2), 83-111.

El-Rashidy, R.A., Grant-Muller, S.M., 2014. An assessment method for highway network vulnerability. *Journal of Transport Geography* 34, 34-43.

Emam, E.B., Al-Deek, H., 2006. Using real-life dual-loop detector data to develop new methodology for estimating freeway travel time reliability. *Freeway Operations and High Occupancy Vehicle Systems* 2006 (1959), 140-150.

Esfeh, M.A., Kattan, L., Lam, W.H.K., Esfe, R.A., Salari, M., 2020. Compound generalized extreme value distribution for modeling the effects of monthly and seasonal variation on the extreme travel delays for vulnerability analysis of road network. *Transportation Research Part C* 120, 102808.

Federal Highway Administration (FHWA), 2006. Travel time reliability: making it there on time, all the time. Report No. 70.

Friesz, T.L., Bernstein, D., Mehta, N.J., Tobin, R.L., Ganjalizadeh, S., 1994. Day-to-day dynamic network disequilibria and idealized traveler information-systems. *Operations Research* 42 (6), 1120-1136.

Garcia-Palomares, J.C., Gutierrez, J., Martin, J.C., Moya-Gomez, B., 2018. An analysis of the Spanish high capacity road network criticality. *Transportation* 45 (4), 1139-1159.

Gedik, R., Medal, H., Rainwater, C., Pohl, E.A., Mason, S. J., 2014. Vulnerability assessment and re-routing of freight trains under disruptions: A coal supply chain network application. *Transportation Research Part E* 71, 45-57.

Guo, R.Y., Yang, H., Huang, H.J., Tan, Z., 2015. Link-based day-to-day network traffic dynamics and equilibria. *Transportation Research Part B* 71, 248-260.

Guo, R.Y., Yang, H., Huang, H.J., Tan, Z., 2016. Day-to-day flow dynamics and congestion control. *Transportation Science* 50 (3), 982-997.

Guo, R.Y., Yang, H., Huang, H.J., 2013. A discrete rational adjustment process of link flows in traffic networks. *Transportation Research Part C* 34, 121-137.

Gu, Y., Fu, X., Liu, Z., Xu, X., Chen, A., 2020, Performance of transportation network under perturbations: reliability, vulnerability, and resilience. *Transportation Research Part E* 133, 101809.

Haghighi, N., Fayyaz, S.K., Liu, X.C., Grubesic, T.H., Wei, R., 2018. A Multi-scenario probabilistic simulation approach for critical transportation network risk assessment. *Networks & Spatial Economics* 18 (1), 181-203.

Han, L.S., Du, L.L., 2012. On a link-based day-to-day traffic assignment model. *Transportation Research Part B* 46 (1), 72-84.

Hazelton, M.L., 2002. Day-to-day variation in markovian traffic assignment models. *Transportation Research Part B* 36 (7), 637-648.
Hazelton, M. L., Parry, K., 2016. Statistical methods for comparison of day-to-day traffic models. *Transportation Research Part B* 92, 22-34.
Hazelton, M.L., Watling, D.P., 2004. Computation of equilibrium distributions of Markov traffic-assignment models. *Transportation Science* 38 (3), 331-342.
He, X.Z., Guo, X.L., Liu, H.X., 2010. A link-based day-to-day traffic assignment model. *Transportation Research Part B* 44 (4), 597-608.
Hensher, D.A., Truong, T.P., 1985. Valuation of travel time savings - a direct experimental approach. *Journal of Transport Economics and Policy* 19 (3), 237-261.
Horowitz, J.L., 1984. The stability of stochastic equilibrium in a two-link transportation network. *Transportation Research Part B* 18 (1), 13-28.
Huang, H.J., Liu, T.L., Yang, H., 2008. Modeling the evolutions of day-to-day route choice and year-to-year ATIS adoption with stochastic user equilibrium. *Journal of Advanced Transportation* 42 (2), 111-127.
Ho, H.W., Sumalee, A., Lam, W.H.K., Szeto, W.Y., 2013. A continuum modeling approach for network vulnerability analysis at regional scale. *Procedia – Social and Behavioral Sciences (Proceedings of the 20th International Symposium on Transportation and Traffic Theory)* 80, 846-859.
Iida, Y., Akiyama, T., Uchida, T., 1992. Experimental-analysis of dynamic route choice behavior. *Transportation Research Part B* 26 (1), 17-32.
Jenelius, E., 2007. Incorporating dynamics and information in a consequence model for road network vulnerability analysis. *The 3rd International Symposium on Transportation Network Reliability (INSTR)*.
Jenelius, E., Mattsson, L.G., 2015. Road network vulnerability analysis: Conceptualization, implementation and application. *Computers Environment and Urban Systems* 49, 136-147.
Kaparias, I., Bell, M.G.H., Belzner, H., 2008. A new measure of travel time reliability for in-vehicle navigation systems. *Journal of Intelligent Transportation Systems* 12 (4), 202-211.
Kitthamkesorn, S., Chen, A., 2013. A path-size weibit stochastic user equilibrium model. *Procedia – Social and Behavioral Sciences (Proceedings of the 20th International Symposium on Transportation and Traffic Theory)* and *Transportation Research Part B* 57, 378-397.
Kitthamkesorn, S., Chen, A., 2014. Unconstrained weibit stochastic user equilibrium model with extensions. *Transportation Research Part B* 59, 1-21.
Kurauchi, F., Ido, H., 2017, Estimation of the expressway/surface road choice model using Logit-Weibit hybrid model. *The 22nd International Conference of Hong Kong Society for Transportation Studies (HKSTS)*.
Li, D., Wu, W., Song, Y., 2020. Comparative study of Logit and Weibit model in travel mode choice. *IEEE Access* 8, 63452-63461.
Li, Y., 2018. Risk assessment of urban backbone road network: A case study of the middle ring accident in Shanghai. Master Thesis, Tongji University.
Liu, Z.Y., Wang, S.A., Zhou, B.J., Cheng, Q.X., 2017. Robust optimization of distance-based tolls in a network considering stochastic day to day dynamics. *Transportation Research Part C* 79, 58-72.
Lo, H.K., Tung, Y.K., 2003. Network with degradable links: capacity analysis and design. *Transportation Research Part B* 37 (4), 345-363.
Lo, H.K., Luo, X.W., Siu, B.W.Y., 2006. Degradable transport network: Travel time budget of travelers with heterogeneous risk aversion. *Transportation Research Part B* 40 (9), 792-806.
Lou, X.M., Cheng, L., Chu, Z.M., 2016. Modelling travellers' en-route path switching in a day-to-day dynamical system. *Transportmetrica B* 5 (1-4), 15-37.
Luathep, P., Sumalee, A., Ho, H.W., Kurauchi, F. 2011. Large-scale road network vulnerability analysis: a sensitivity analysis based approach. *Transportation* 38 (5), 799-817.
Mattsson, L.G., Jenelius, E. 2015. Vulnerability and resilience of transport systems - A discussion of recent research. *Transportation Research Part A* 81, 16-34.
Meneguzzer, C., 2012. Dynamic process models of combined traffic assignment and control with different signal updating strategies. *Journal of Advanced Transportation* 46 (4), 351-365.
Mirchandani, P., Soroush, H., 1987. Generalized traffic equilibrium with probabilistic travel-times and perceptions. *Transportation Science* 21 (3), 133-152.

Murray, A.T., Grubesic, T.H., 2007. *Critical infrastructure: reliability and vulnerability*. Springer-Verlag, Berlin, Heidelberg.

Nagurney, A., Qiang, Q., 2010. *Fragile networks: identifying vulnerabilities and synergies in an uncertain world*. John Wiley & Sons, Inc.

Oliveira, E.L., Portugal, L.D., Porto, W., 2016. Indicators of reliability and vulnerability: Similarities and differences in ranking links of a complex road system. *Transportation Research Part A* 88, 195-208.

Rakha, H., El-Shawarby, I., Arafeh, M., 2010. Trip travel-time reliability: issues and proposed solutions. *Journal of Intelligent Transportation Systems* 14 (4), 232-250.

Rambha, T., Boyles, S.D., 2016. Dynamic pricing in discrete time stochastic day-to-day route choice models. *Transportation Research Part B* 92, 104-118.

Reggiani, A., Nijkamp, P., Lanzi, D., 2015. Transport resilience and vulnerability: The role of connectivity. *Transportation Research Part A* 81, 4-15.

Sheffi, Y., 1985. Urban Transportation Network. Pretince Hall.

Shen, L., Shao, H., Wu, T., Fainman, E.Z., Lam, W.H.K. 2020. Finding the reliable shortest path with correlated link travel times in signalized traffic networks under uncertainty. *Transportation Research Part E* 144, 102159.

Smith, M.J., 1983. The existence and calculation of traffic equilibria. *Transportation Research Part B* 17(4), 291-303.

Smith, M.J., 1984. The stability of a dynamic model of traffic assignment-an application of a method of Lyapunov. *Transportation Science* 18 (3), 245-252.

Tan, Z., Yang, H., Guo, R.Y., 2015. Dynamic congestion pricing with day-to-day flow evolution and user heterogeneity. *Transportation Research Part C* 61, 87-105.

Taylor, M.A.P., 2017. *Vulnerability analysis for transportation networks*. Elsevier.

Tian T.T., Chen, X.H., 2019. Analysis of the impact of the Shanghai Central Accident based on the macroscopic fundamental diagram. *Proceedings of the 2019 China Urban Transportation Planning Annual Conference*. 3712-3725.

Tinessa, F., Simonelli, F., Marzano, V., Buonocore, C., 2020. Evaluating the choice behaviour of high-speed rail passengers in Italy: a latent class structure with alternative kernel models to the Multinomial Logit. *2020 IEEE International Conference on Environment and Electrical Engineering and 2020 IEEE Industrial and Commercial Power Systems Europe (EEEIC / I&CPS Europe)*.

van Lint, J.W.C., van Zuylen, H.J., Tu, H., 2008. Travel time unreliability on freeways: why measures based on variance tell only half the story. *Transportation Research Part A* 42 (1), 258-277.

Watling, D., Hazelton, M.L., 2003. The dynamics and equilibria of day-to-day assignment models. *Networks & Spatial Economics* 3 (3), 349-370.

Watling, D.P., Cantarella, G.E., 2015. Model representation & decision-making in an ever-changing world: the role of stochastic process models of transportation systems. *Networks & Spatial Economics* 15 (3), 843-882.

Wan, C., Yang, Z., Zhang, D., Yan, X., Fan, S., 2018. Resilience in transportation systems: a systematic review and future directions. *Transport Reviews* 38, 479-498.

Wang, G.T., 2019. Introduction of the urban mobility. Shanghai: Tongji University Press.

Wang, Y., Liu, H., Han, K., Friesz, T.L., Yao, T., 2015. Day-to-day congestion pricing and network resilience. *Transportmetrica* 11 (9-10), 873-895.

Wang, D.Z.W., Liu, H.X., Szeto, W.Y., Chow, A.H.F., 2016a. Identification of critical combination of vulnerable links in transportation networks - a global optimisation approach. *Transportmetrica A* 12 (4), 346-365.

Wang, D.Z.W., Nayan, A., Szeto, W.Y. 2018. Optimal bus service design with limited stop services in a travel corridor. *Transportation Research Part E* 111, 70-86.

Wang, J., He, X.Z., Peeta, S., 2016b. Sensitivity analysis based approximation models for day-to-day link flow evolution process. *Transportation Research Part B* 92, 35-53.

Wardrop, J.G., 1952. Some theoretical aspects of road traffic research. *Ice Proceedings Engineering Divisions* 1 (3), 325-362.

Wen, K., Xie, J., Chen, A., Wong, S.C., Zhan, S., Lo, S.M., Qiang, L. 2021. Empirical analysis of scaled mixed itinerary-size weibit model for itinerary choice in a schedule-based railway network. *Transportmetrica A: Transport Science*, 1-29.

Xiao, F., Yang, H., Ye, H.B., 2016. Physics of day-to-day network flow dynamics. *Transportation Research Part B* 86, 86-103.

Xiao, F., Shen, M., Xu, Z., Li, R., Yang, H., Yin, Y., 2019. Day-to-day flow dynamics for stochastic user equilibrium and a general Lyapunov function. *Transportation Science* 53 (3), 683-694.

Xu, X., Chen, A., Cheng, L., Lo, H.K., 2014. Modeling distribution tail in network performance assessment: A mean-excess total travel time risk measure and analytical estimation method. *Transportation Research Part B*. 66, 32-49.

Xu, X., Chen, A., Cheng, L., Yang, C., 2017. A link-based mean-excess traffic equilibrium model under uncertainty. *Transportation Research Part B* 95, 53-75.

Xu, X., Chen, A., Jansuwan, S., Yang, C., Ryu, S., 2018a. Transportation network redundancy: Complementary measures and computational methods. *Transportation Research Part B* 114, 68-85.

Xu, X., Chen, A.,Yang, C., 2018b. An optimization approach for deriving upper and lower bounds of transportation network vulnerability under simultaneous disruptions of multiple links. *Transportation Research Part C* 94, 338-353.

Yang, F., Zhang, D., 2009. Day-to-day stationary link flow pattern. *Transportation Research Part B* 43 (1), 119-126.

Yang, H., Bell, M.G.H., 1998. Models and algorithms for road network design: a review and some new developments. *Transport Reviews* 18 (3), 257-278.

Yang, X., Chen, A., Ning, B., Tang, T. 2017. Bi-objective programming approach for solving the metro timetable optimization problem with dwell time uncertainty. *Transportation Research Part E* 97, 22-37.

Ye, H.B., Xiao, F., Yang, H., 2018. Exploration of day-to-day route choice models by a virtual experiment. *Transportation Research Part C* 94, 220-235.

Ye, H.B., Xiao, F., and Yang, H., 2021. Day-to-day dynamics with advanced traveler information. *Transportation Research Part B* 144, 23-44.

Yu, Y., Han, K., Ochieng, W., 2020. Day-to-day dynamic traffic assignment with imperfect information, bounded rationality and information sharing. *Transportation Research Part C* 114, 59-83.

Zhang, D., Nagurney, A., Wu, J.H., 2001. On the equivalence between stationary link flow patterns and traffic network equilibria. *Transportation Research Part B* 35 (8), 731-748.

Zhou, B.J., Xu, M., Meng, Q., Huang, Z.X., 2017. A day-to-day route flow evolution process towards the mixed equilibria. *Transportation Research Part C* 82, 210-228.

Zhou, Y., Wang, J., Yang, H., 2019. Resilience of transportation systems: concepts and comprehensive review. *IEEE Transactions on Intelligent Transportation Systems* 20 (12), 4262-4276.

Zhu, Z., Zhu, S.J., Zheng, Z.F., Yang, H., 2019. A generalized Bayesian traffic model. *Transportation Research Part C* 108, 182-206.